Design of a high speed soft robotic fish

S. C. van den Berg

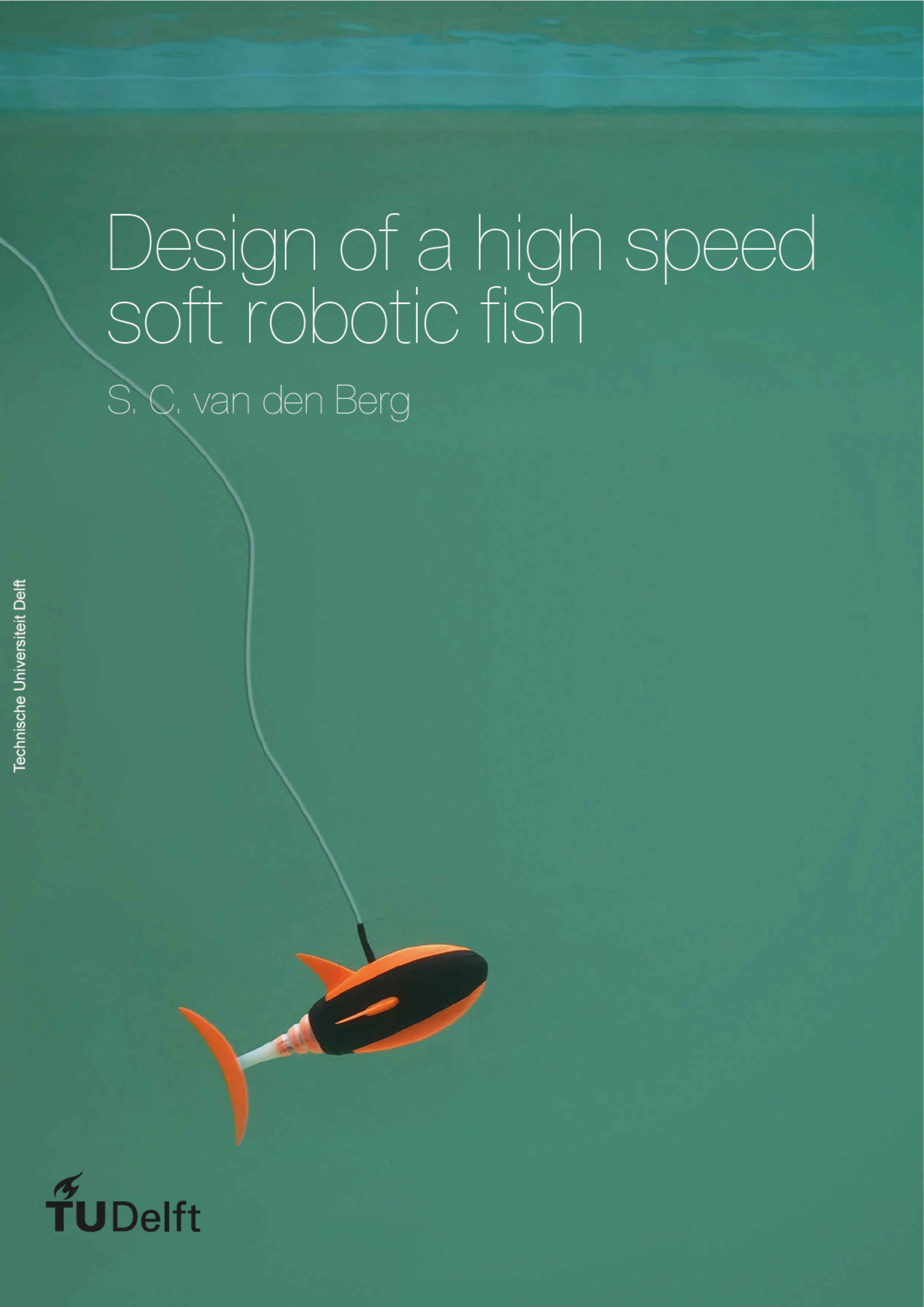

Technische Universiteit Delft

Design of a high speed soft robotic fish

by

S. C. van den Berg

to obtain the degree of Master of Science
at the Delft University of Technology,
to be defended publicly on Friday July 19, 2019 at 10:45 AM.

Student number:	4172272	
Thesis committee:	dr. J. Rusák,	TU Delft, chair
	Dr. ir. j. Wu,	TU Delft, mentor
	Msc. R.B.N. Scharff,	TU Delft, 2nd mentor

This thesis is confidential and cannot be made public until July 19, 2019.

TU Delft

Contents

1

Summary

We present a novel DC motor driven soft robotic fish and optimization based on experimental, numerical and theoretical investigation into oscillating propulsion for primarily speed and secondarily efficiency. Our system outperforms the previously fastest soft robotic fish Zhong et al. 2017[29] by a significant margin of 27%, with speeds upto 0.85m/s. A simple wire-driven active body and soft compliant body were used to mimic highly efficient thunniform swimming. The efficient DC motor to drive the system decreases internal losses compared to other soft robotic oscillating propulsion systems which are driven by one or multiple servo motors. The DC motor driven design allows for swimming at higher frequencies. The current design has been tested up to 5.5 Hz but can potentially reach much higher frequencies.

2

Acknowledgements

During my thesis project I needed to venture into for me previously unexplored educational areas, extending my knowledge in hardware, software and biology. I could not have obtained the results I have without the expert guidance and support of the people around me.

I would like to thank my supervisors, Zoltán Rusák, Jun Wu and Rob Scharff, who helped me steer the project in the right direction, gave critical feedback and supported me throughout this project. I would like to thank Bas Gores, who with his experience with O-foil taught me so much and was willing to take significant time to help me better understand oscillating propulsion from a biological perspective. Tim Vercruyssen for sharing his experience with the Galatea robot and guiding me to resources of the TUD giving me a head-start. Peter Poot for allowing me to use the 3ME towing tank for testing. Viki Pavlic of the course Build Your Start-up and Tommie Perenboom who was my groupmate during the course for helping me find and understand the market potential of oscillating marine propulsion. Wiebe Draijer of the PMB, Martin Verwaal and Adrie Kooijman of Applied Labs and Frits Sterkof from 3ME for sharing their knowledge on electronics helping me tankle the many issues I encountered. Wijnand van Oosten of fish shop W W Van Oosten for helping me obtain different fishtails to test. Sepideh Ghodrat for guiding me in my material selection.

And most of all the TU Delft itself and the faculty who supported this project by means of the start-up voucher, allowing me to research and validate this technology. I would not have been able to get this project off the ground without their trust and financial support.

3 Introduction

The past three decades a large amount of research has been done on investigating oscillating propulsion systems. Although high efficiencies of up to 87% [2] have been reported in experiments with pitching and heaving foils, the complexity of the mechanisms has prevented the implementation of oscillating propulsion in the market. The designs generally consist either of multilink servos or multiple motors controlling the pitch and heave of a foil. Recently research has shown a single servo driven oscillating propulsion system with a compliant and active tail part[29]. This research could be the basis of a much simpler compliance based oscillating propulsion system.

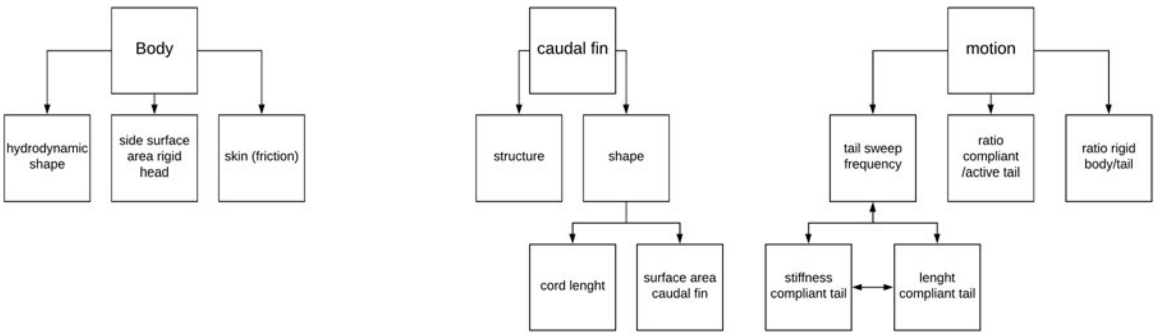

Figure 3.1: Overview of identified design variables for a compliancy based oscillating propulsion system

In this thesis we investigate the influence of different aspects of the motion, propulsor and body of a compliance based oscillating propulsion system on locomotive speed. The identified variables can be found in fig. 3.1. Although identified both caudal fin structure and skin friction have not been taken into account in this thesis to limit the research scope.

The goal of this project is to showcase the possibilities of oscillating propulsion for (under)water crafts by generating high speed with relatively low complexity.

3.1. Background and related work

To understand the context of oscillating propulsion for a historical overview is created of robotic fish. Showcasing their accomplishments but also their limitations. This overview also leads to conclusions and design decisions for our robotic fish.

Table 3.1: Overview of previous robotic fish and their achievements on speed. Green highlighted are soft robots, orange highlighted are robots using rotary shaft systems.

Name	University	Year of pub.	Max. speed BL/s	Max. speed (m/s)	Frequency (hz)	Body	Source
Barrett's RoboTuna	MIT	1999	0.65	0.7	1.1	8 links multilink, not free swimming	Barret et al. 1999
Kumph's robotic pike	MIT	2000	0.1	0.09	1	Multilink (5 links),external motors	Kumph et al. 2000
UPF-2001	NMRI Japan	2001	1	1	10	Multilink (3 link)	Hirata & Kawai, 2001
Anderson's VCUUV robotictuna	Cambridge, massachusetts	2002	0.5	1.2	1	Hydraulic multilink	Anders et al. 2002
y Alvarado's compliant assembly	MIT	2003	0.6	0.095	4	Compliant body, not free swimming	y Alvarado et al. 2003
Yu's carangiform swimmer	Chinese Academy of Sciences	2004	0.8	0.32	2	multilink	Yu et al. 2004
Compliant Robotic Tuna	MIT	2008	0.37	0.1	2	Compliant body	Mazumdar et al. 2008
Liu's G9 carangiform swimmer	University of Essex	2010	1.02	0.5	1.3	multilink	Liu et al. 2010
Isplash 1	University of Essex	2014	2.8	0.7	6.6	Multilink rotary shaft	Clapham et al. 2014
Isplash 2	University of Essex	2015	11.6	3.7	20	Multilink rotary shaft	Clapham et al. 2015
Zhong activecompliant	University of Hong Kong	2017	2.15	0.67	3	compliant/active body, soft robotic	Zhong et al. 2017
SoFi	MIT	2018	0.51	0.235	1.4	Hydraulic soft robotic system	Katzschmann et al. 2018
Robofish S-tail	**TU Delft**	**2019**	**1.81**	**0.74**	**2.68**	**compliant/active body, soft robotic**	
Robofish L-tail	**TU Delft**	**2019**	**2.05**	**0.85**	**5.46**	**compliant/active body, soft robotic**	

3.1.1. RoboTuna and multilink propulsion

MIT's RoboTuna is one of the first and therefore probably also one of the most well known robotic fish. It was built to investigate oscillating propulsion as an alternative means for propulsion for Autonomous Underwater Vehicles. The project started in 1993 and continued in multiple forms still at MIT but the main project moved to Franklin W. Olin College of Engineering and continues to this day under the name GHOSTswimmer at Boston Engineering. Early on the robot turned out to be more maneuverable and used less energy than other AUV's at the time, helping the research to acquire significant funding which allowed the project to continue to this day.

RoboTuna originally propelled itself by series of pulleys pulled by external motors which were connected outside the body through a mast on top to a carriage mount. It therefore could not swim freely. Later versions kept the same system but with smaller motors placed inside. After some more adaptations this allowed the versions at Franklin W. Olin College of Engineering to swim freely.

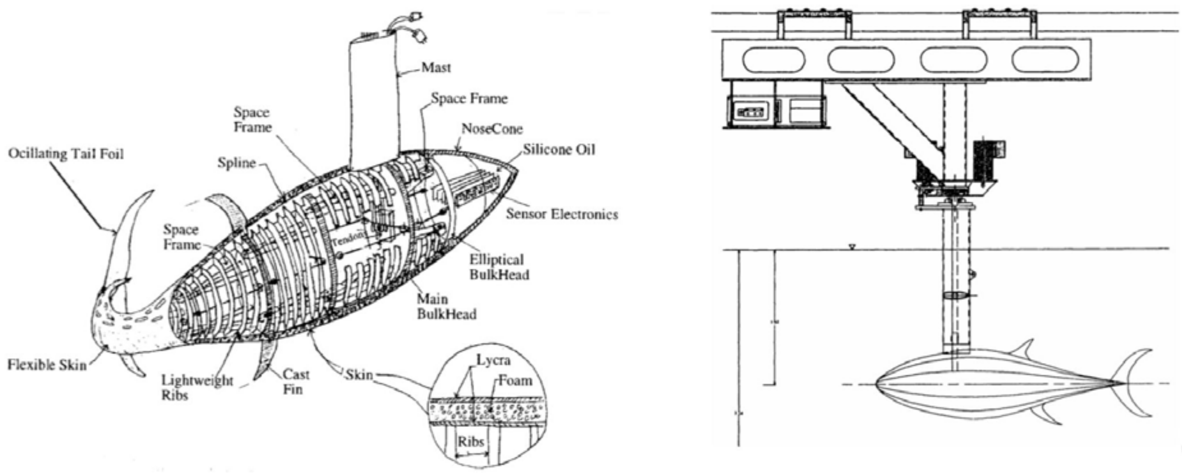

(a)

(b)

Figure 3.2: RoboTuna inside (a) and sideview of carriage mount (b). Reproduced from SW Tolkoff, 1999[21]

.

RoboTuna's success was most likely to thank due to its complex pulley system allowing it to very precisely mimic the motion described by previously executed research on live tuna and heaving and pitching foils. Due to this success it was used as a reference for most robotic fishes for the next 10 years. But this multilink system has also some large drawbacks.

Although the movement can be made pretty efficient, the internal loses are huge due to the amount of transmissions needed, it is very expensive due to the amount of motors needed and due to the complexity, most of the body is filled with the propulsion system itself not allowing any payload to be taken with it for any practical application. Although promising no real life implementation occurred except significant military interest.

3.1.2. Compliant body

In 2003 y Alvarado[28] published a paper based on a compliant tail segment, meaning the tail was meant to bend to create the desired motion. This significantly reduced the complexity and therefore also the cost of such a robotic oscillating system. The initial positive results can however be taken with a grain of salt. As based on the ratio between active and compliant tail this robotic fish would never have swum if it was not held straight due to the connected mast and carriage mount. However building further on this concept Mazumdar built a free swimming fish in 2008 [19]. Due to only having a compliant body part it makes quite a sharp angle between the activated segment and passive segment slowing it down.

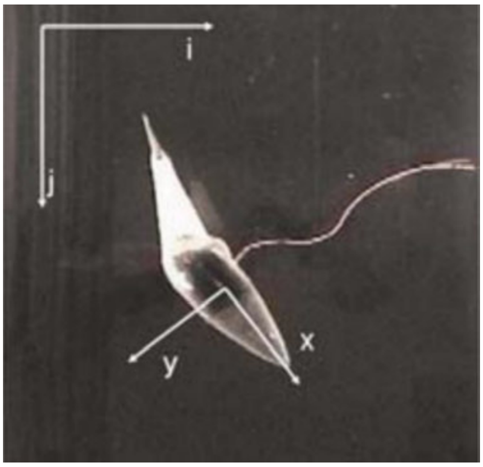

Figure 3.3: Mazumdar compliant robotic tuna, showcasing the sharp angle it makes between the passive head and compliant tail. Reproduced from Mazumdar et al. 2008[19]

.

3.1.3. Compliant & active tail

The compliant active tail design enables a smooth transition between the rigid head and compliant tail. This enables a more streamlined body better allowing the creation of a reverse von karman vortex (see chapter 4.1. How fish swim), similar to the compliant body design this design only requires one motor enabling it to be hugely more efficient internally compared to the earlier multilink design. Taking into account the results on speed, and reduction on complexity this design is a big step towards a viable system.

3.1.4. Multilink rotary shaft

Multilink rotary shaft propulsion is a bit of an outlier. It has been applied in one of the versions of the RoboTuna once and was implemented by Clapham in his Isplash concepts [5][6]. The largest benefit of this design is that the motion of the robot stays the same for any tail beat frequency. Allowing testing up to very high frequencies without large modifications. This concept also proved what was already shown in fish, that when tail beat frequency increases above a certain threshold (around 5 Hz) the speed increases in a power law relation.

However this design also has some major drawbacks, it is very prone to wear, needs high precision fabrication to be created and does not allow for any easy steering mechanism. These limitations make it not useful for any practical application

3.1.5. Conclusion

Multilink	Advantages	Disadvantages
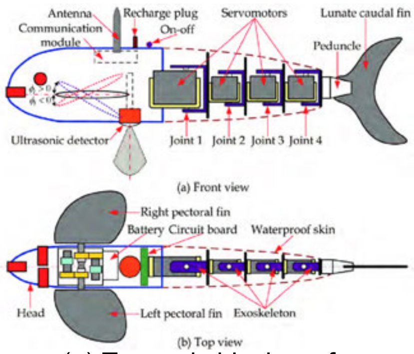 (a) Top and sideview of a multilink prototype. Reproduced from Jia & Wang 2014 [12]	• Good control incl. Steering	• Expensive (multi servo) • Low frequency • Low internal efficiency
Multilink rotary shaft (single DC motor)	**Advantages**	**Disadvantages**
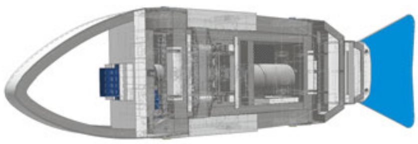 (b) Isplash optimize, example of a multilink rotary shaft design. Reproduced from Clapham 2016[7]	• Easily enables high tail beat frequency • High speed	• Does not enable steering • Expensive precision fabrication needed • Prone to wear
Compliant body	**Advantages**	**Disadvantages**
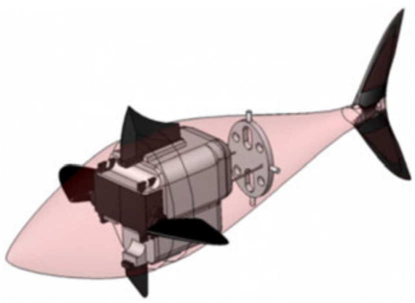 (c) Mazumdar compliant robotic tuna. Reproduced from Mazumdar et al. 2008[19]	• Cheap • Simple	• Low frequency • Low efficiency
Compliant & active body (single servo)	**Advantages**	**Disadvantages**
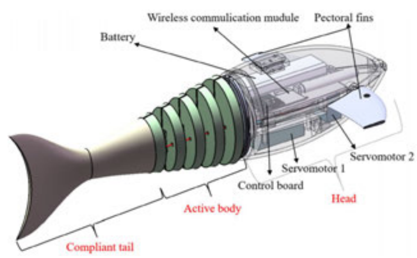 (d) Zhong's active/compliant body robotic fish. Reproduced from Zhong et al. 2017 [29]	• Cheap • Simple • Good control incl. Steering • High efficiency possible	• Only highly efficient at one tail beat frequency

The compliant active tail design was selected to work further upon. This design shows the most potential for the future. As we design for speed a design challenge will be to increase the tail beat frequency above 3 Hz as servo's (the motors used to control these robots) generally do not go above 3 Hz. Requiring a new approach to enable increased frequencies yet to be designed. A multilink rotary shaft system was not chosen as this system has very limited practical application mostly due to being very prone to wear and the specialized precision fabrication needed to fabricate the system.

3.2. Benefits and challenges

Figure 3.4: Overview of most important benefits of oscillating propulsion. Figure made by Tommie Perenboom.

Oscillating propulsion has a few major benefits. One of the main drivers for research is its potential to be more efficient than traditional rotary propulsion. Specifically at relatively low speeds oscillation can be very efficient. Wherein rotor blades are generally very inefficient at low speeds. Small propellers used to drive underwater vehicles typically do not produce efficiencies above 40% (Triantafyllou et al. 1995[23]). Where oscillating in lab experiments have shown efficiencies of up to 87% (Anderson et al. 1998[2]). Thus oscillation showing a potential increase of efficiency of more than 100%.

Oscillation also has better performance at high depth further increasing its efficiency compared to conventional propellers. In a conventional propeller driven craft the propeller shaft goes through a hole in the body, through this gap water could seep through. To combat this in rotary propulsion large pressure is exerted on the rotary shaft at high depths, greatly reducing its efficiency. An oscillating system lacks external rotating components enabling complete encapsulation.

Due to the lower frequency of movement far fewer vibrations are emitted, making crafts nearly undetectable and indistinguishable from fish. The soft tale, lack of sharp edges and slower motion make the propulsion system also very safe. And ropes, debree and plants get less easily entangled in an oscillating propulsion system.

There are of course also some drawbacks. The inherent swaying motion of oscillation can be undesirable for many purposes. This could be countered by 2 opposite moving flapping tails or a sail similar to sailfish (Stefano Marras et al. 2015[18]). 4 flapping tails would also counter the inconsistent speed. The complexity and associated cost might not offset its benefits such as higher efficiency in many commercial markets. Therefore the highest chance of early acceptance might be in markets where a small benefit in the identified benefit areas justifies a high increase in cost, such as stealth for military, high depth efficiency for deep sea mining and pipeline inspection and silence and safety for aquatic research purposes.

4

Literature study

4.1. How fish swim

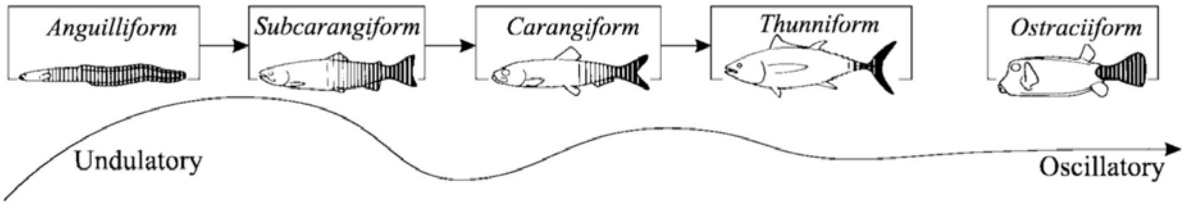

Figure 4.1: the most common body/caudal fin swimming mode categories. Shaded areas contribute to thrust generation. Reproduced from Lindsey [17].

Fish motion can be separated into 5 main categories, which are mainly separated by their ratio of active thrust producing body versus passive rigid head. For our robotic fish a thunniform swimming motion is chosen to be mimicked as closely as possible. This decision was based on the following benefits:

- Thunniform swimming is widely known to be very efficient and adopted by most prolonged fast swimmers.

- Thunniform swimming exhibits the least lateral movement of the head, creating a more stable motion.

- In comparison with carangiform, subcarangiform and anguilliform swimming, thunniform swimming has proportionally a large passive body in relation to the undulatory moving tail. This enables larger space for payloads such as sensors, actuators and power supply.

The biggest drawback from thunniform swimming is limited maneuverability compared to other modes of aquatic locomotion.

Most modes of aquatic locomotion and especially highly efficient ones like thunniform oscillating locomotion work by creating inwards turning vortices on both sides which produce a peak thrust in the middle behind an aquatic animal. This is called a reverse karman vortex.

Less efficient swimming modes like ostraciiform and carangiform motion use this reverse von karman vortex creation to a lesser extent. Their thrust is created more based on simple reaction forces making it easier to model, predict and reproduce. It is assumed that using a combination of numerical and experimental research the swimming motion of our robotic fish can be optimized to a highly efficient thunniform swimming motion.

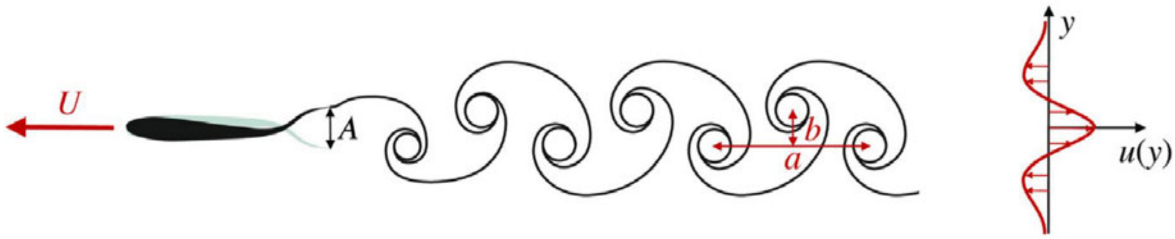

Figure 4.2: Illustration of inwards turning vortices creating thrust behind the fish. Reproduced from Eloy [8].

Figure 4.3: Fish schooling pattern. Reproduced from Ashraf et al. [3].

4.2. Schooling

The von karman vortex can be used for schools of (robotic) fish to swim even more efficient. As can be seen at figure 4.2 at the side of the reverse von karman vortex street a forward thrust is generated. This due to the rotating vortices. If two fish swim side by side this forward thrust generation is even stronger. These are the forces that keep schooling fish together. Between the fish there is a forward pushing stream and directly behind the fish there is a wall of a backwards pushing stream. Because the vortices rotate towards the forward pushing stream schools of fish are able to swim in tight schools with very high efficiency. The efficiency of such a vortex street in a school can be so strong that it captures dead fish in a school [14]. Birds also use these vortices to fly more efficiently in a V or diamond formation.

4.3. Body kinematics for fast efficient swimming

In this chapter we investigate the theoretical optimum body kinematics for efficient and fast swimming. From this theory we derive goals for parameters such as tail angle of attack and a frame of reference for the performance of our robotic fish. The desired characteristics of the tail are investigated in a separate subsection (Propulsor (Caudal fin)).

4.3.1. Efficiency

The strouhal number is a dimensionless number which describes the relation between the sweeping frequency and amplitude in relation to the swimming speed.

$$St = fA/U$$

where, for fish, f is tail beat frequency (Hz), A is peak-to-peak stroke amplitude of the tail tip (m), and U is equal to swimming speed (m/s).

Large quantities of research have shown that all oscillating propulsive animals cruise at the same narrow interval of $0.2 < St < 0.4$, such as dolphins, sharks, bony fish but also birds, bats and insects (Taylor et al. 2003[20]). Because natural selection is likely to tune animals for high propulsive efficiency it is assumed that the highest propulsive efficiency is in this range.

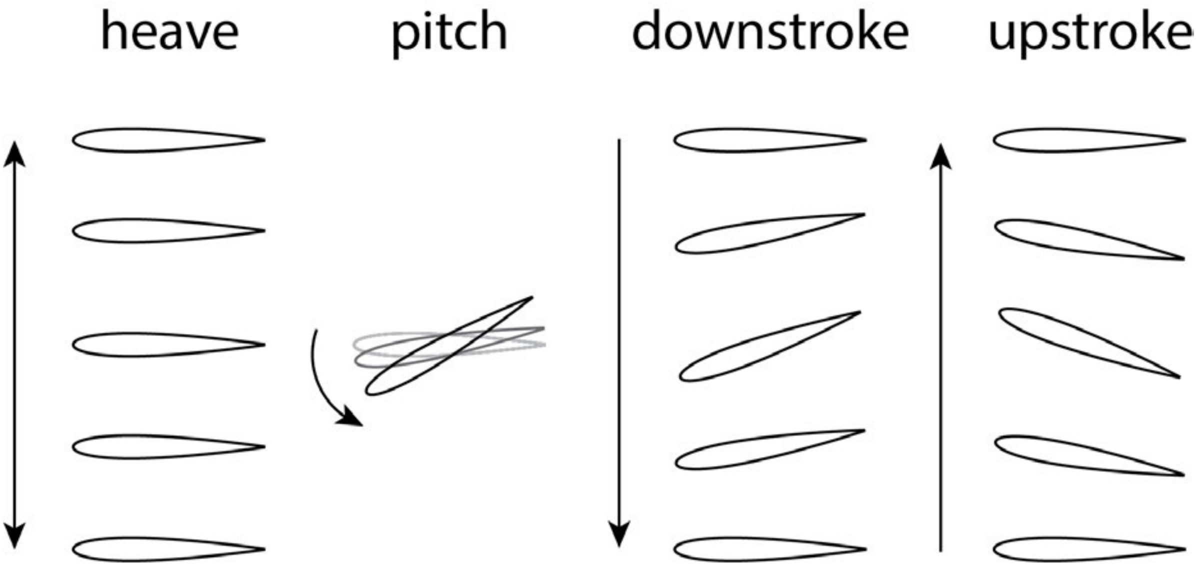

Figure 4.4: Diagram showcasing heave and pitch in a heaving and pitching foil system.

Experiments with pitching and heaving foils confirmed this suspicion. In an experiment with a pitching and heaving 0012 NACA profile the highest propulsive efficiency was measured at a strouhal number of 0.25 (Triantafyllou et al. 1993[22]). Another researcher with a similar set-up witnessed the highest recorded efficiency at 87% obtained at a St = 0.30 and tip to tip strouhal of $St_{TE} = 0.36$ (Anderson et al. 1998[2]). St here defined as the heave distance of the foil and St_{TE} as the tip to tip excursion of the tip of the foil. Which is not per definition the same if the foil is at an angle at its maximum heave distance.

Notably the highest efficiency in this experiment was obtained at the highest tested heave amplitude to chord ratio of 0.75. Indicating a large amplitude with a small caudal fin chord length is preferred. Maximizing the heave amplitude in the oscillating movement should therefore be strived for. The maximum angle was 20.2° with the direction of movement during the experiment with the highest efficiency. This is in line with previous research indicating an ideal maximum angle of attack of between 15° and 25° (Triantafyllou and Triantafyllou 1995[23]).

In conclusion, for high efficiency a motion should be strived for that makes a maximum angle and strouhal number of approximately 20° and 0.3 respectively.

4.3.2. Speed limitations

To obtain realistic insight in the top speed reachable by oscillating propulsion we looked into both theoretical and experimental evidence of top speeds and cruising speeds of marine fish. Due to cavitation problems, theoretical work suggests that the maximum speeds attainable by marine fish and cetaceans (marine mammals) are limited to 10–15m/s at shallow depths (Iosilevskii and Weihs 2007[11]). Using high speed video footage and accelerometry of sailfish, (often assumed to be the fastest swimming fish) showed a mean cruising speed of 2.30 ±

0.1m/s and 7.02 ± 0.48m/s mean speed at burst (Marras et al. 2015[18]), well within the theoretical maximum.

4.4. Propulsor (Caudal fin)

The caudal fin is the main generator of propulsive force. Therefore the design of the caudal fin is of high importance to the resulting swimming motion both in efficiency and thrust.

Most fish use the caudal fin not only as the main source for propulsive force but also for steering. In different species it is optimized to create the characteristics which provide the highest chance of survival for that species. For coral fish, fast swimming is for instance not a necessity but fast acceleration and maneuverability is an important property to be able to hide quickly from predators in the crevices of the coral reef. These fish need flexible and highly adjustable tails (Videler 2012[25]). In this chapter we will focus on caudal fins generating efficient high speed.

4.4.1. General shape

As the focus of this project is efficiency and speed we focus on the morphology of fast ocean going species. Because there are little to no obstacles in the open ocean pelagic swimmers have specialized speed over agility. These fast swimming fish have a much stiffer tail, the tail is symmetric, lunate shaped with large spans and small chords (see section chord ratio for more information).

The lunate shape is important for its performance. In experiments the backwards curving leading edge reduced drag by 8.8% compared to a wing with the same chord ratio with a straight leading edge (Westerhoff et al. 1987[27]).

Table 4.1: Illustration of different caudal fins retrieved from: https://www.koaw.org/caudal-fin-types

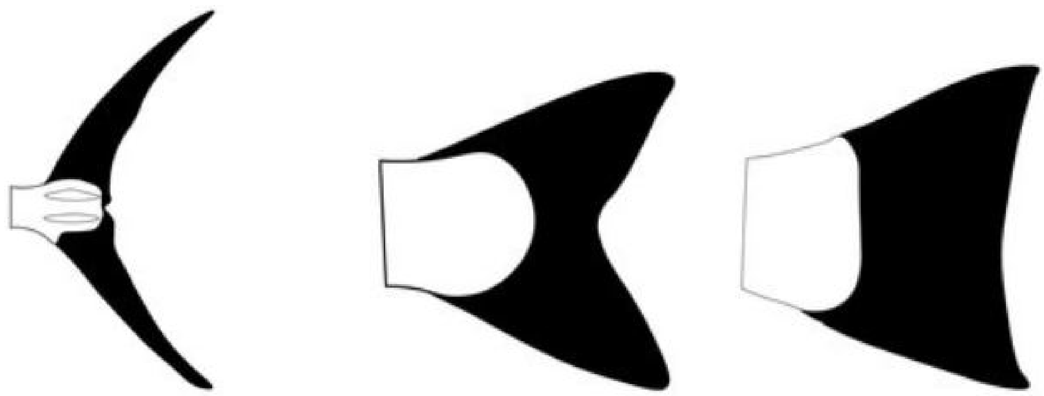

Tail shape	Lunate	Emarginate and forked	Truncate and rounded
function	High efficiency, high speed cruising, low maneuverability	Good speed cruising, medium maneuverability	Very high acceleration and maneuvering (from standstill) but high drag and at highspeeds, tired fast. Cruises at low speeds.

4.4.2. Chord ratio

The chord ratio or in aeronautics generally referred to as just the aspect ratio is the ratio between the wing or in our case caudal fin length to its mean chord length. The lift/thrust-to-drag ratio increases with chord ratio, meaning the higher the tail relative to its length the more efficiently it swims (Kermode 1987[13]). This is general knowledge for fixed wing aeroplanes.

It works as follows: a pressure difference is generated between each side of the hydrofoil. The pressure difference generates vortices at the tip of the tail. The energy put in creating these vortices dissipates and produces drag as it is not used to generate thrust. The vortices at high tails (and long wings in flight) are smaller compared to the total length over which the pressure difference is maintained. Resulting in a higher efficiency. (Videler 2012[25])

Validation can also be found in nature. Long maintained fast swimming fish and birds have high aspect ratio such as sailfish, albatrosses and eagles. By contrast highly maneuverable fish and birds have a low aspect ratio, examples are reef fish, hummingbirds and the sparrowhawk. A very low aspect ratio is beneficial for high acceleration but limits it total swimming speed and efficiency. This type of caudal fin can be witnessed in ambush predatory fish like pike.

As mentioned in the chapter 4.1 How fish swim Anderson et al. 1998[2] shows this to be true not only for static but also for heaving and pitching foils as the highest efficiency was obtained when the heave amplitude-to-chord ratio was at its highest tested value.

4.5. Flexibility

Figure 4.5: Photograph showing the deformation of the caudal fin is higher in the middle of the fin due to lower stiffness. Reproduced from Jervis Bay Wild https://twitter.com/jervisbaywild.

Research on the effects and importance of flexibility has been limited, and knowledge in this area is still largely based on assumptions and theories based on limited evidence and thus this topic should be approached with some caution.

All fish have caudal fins consisting of fin rays, aquatic mammals like dolphins and whales do not. These fin rays are connected to tendons which allows these fish to adjust the movement and shape of the caudal fin to some degree. Highly maneuverable fish have better control over these fin rays than pelagic swimmers like tuna and swordfish.

An electromyography of a tilapia, a highly maneuverable fish, shows that intrinsic caudal fin muscles are active up to 65% of the time during swimming strokes (videler 1975[24]). The intrinsic caudal fin muscles exert a force on the fin ray heads. This bends the caudal fin in the opposite direction as the forces. Creating a scoop shape. The connection between the vertebral column and fin ray head fulfills two incompatible functions. It needs to be highly adjustable if maneuverability is required and fairly stiff to transfer large forces to provide thrust. In tuna a clear preference is present for stiffness as the fin ray heads completely overlap the ural plate connecting directly to the last vertebral body. The propulsive forces are therefore transmitted directly in a bone to bone connection leaving no adjustability of the fin rays. This is most probably the case in all lunate tail shaped pelagic swimmers. These tails however still exhibit some deformation towards the direction of force suggestive there is also a passive element of this caudal fin deformation (lauder 2006[15]). How this mechanism works in unknown, but it has been reproduced mechanically showing how it might work. An example of such a system made of paper is exhibited in fig. 4.6.

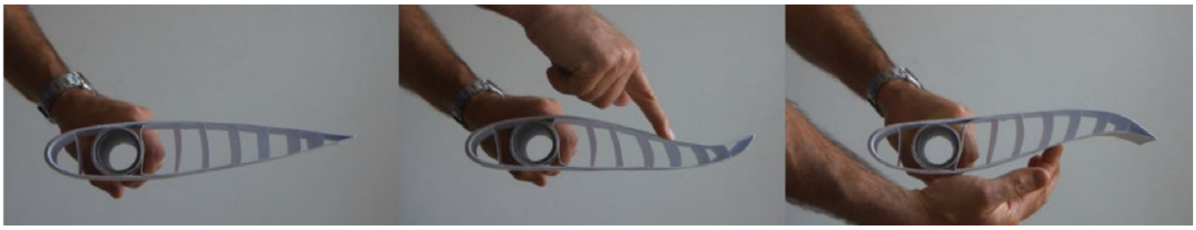

Figure 4.6: Research by Bas Goris at O-foil shows a paper construction creating the shape modifying characteristics of passive fin rays. Pressure bends the fin in the direction of pressure. The created camber increases the maximum thrust coefficient. Reproduced from https://vimeo.com/22887842.

Aquatic mammals also exhibit some flexibility in their tales according to Frank Fish, a marine biologist at West Chester University in Pennsylvania in an article by Jane J. Lee in National Geographic (2014). According to Fish this flexibility is key to the enable dolphins to maintain a highly efficient way of swimming. In the article he suggests these aquatic mammals might be able to adjust the stiffness of their caudal fin enabling them to swim very efficient at different speeds. Fish does however explicitly mentions he is not sure how and if they adjust the stiffness.

4.6. Stability

The first prototype showed significant instability. Most notable significant yaw of the head which dissipated energy creating a prototype which produced almost no thrust. This chapter is a theoretical investigation into what causes instability. Based on this chapter new numerical experiments and prototypes are build to validate these insights and improve the prototype design.

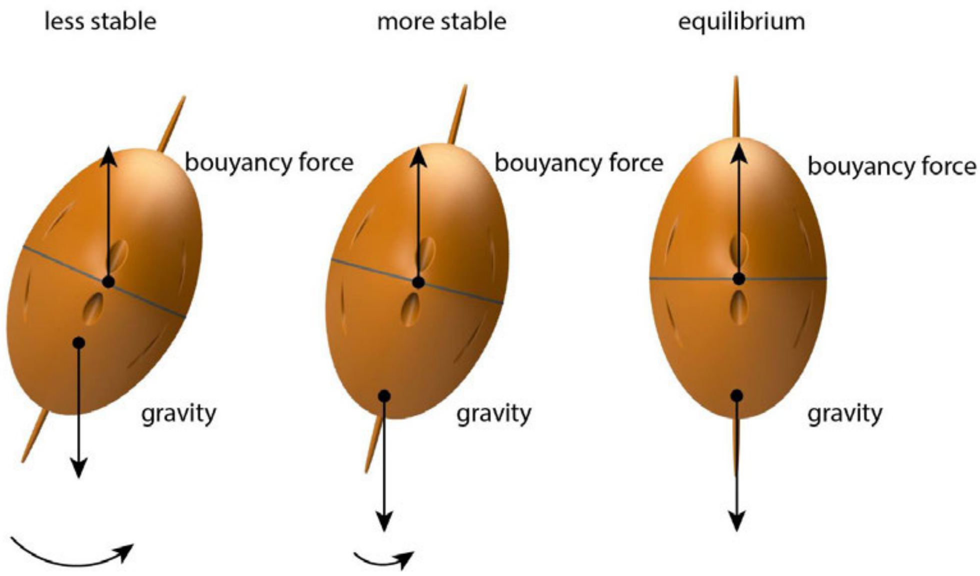

Figure 4.7: Stability illustration depicting the influence of placement of center of gravity on stability

4.6.1. Static stability

An object submerged or floating in a fluid will rotate to align the center of gravity below the center of buoyancy. The center of gravity is the center of the weight of the object. The center of buoyancy is the center of gravity of the fluid volume displaced. In our prototypes the center of gravity is adjusted with adhesive lead so the prototype is suspended in a horizontal position.

When forces are applied to try to rotate the object the object it will rotate around the center of buoyancy. The longer the distance (arm) between the center of buoyancy and center of gravity the more force is needed for the body to roll or pitch making it more stable. E.g. mass should be placed as low as possible in the object.

4.6.2. Yaw and roll stability

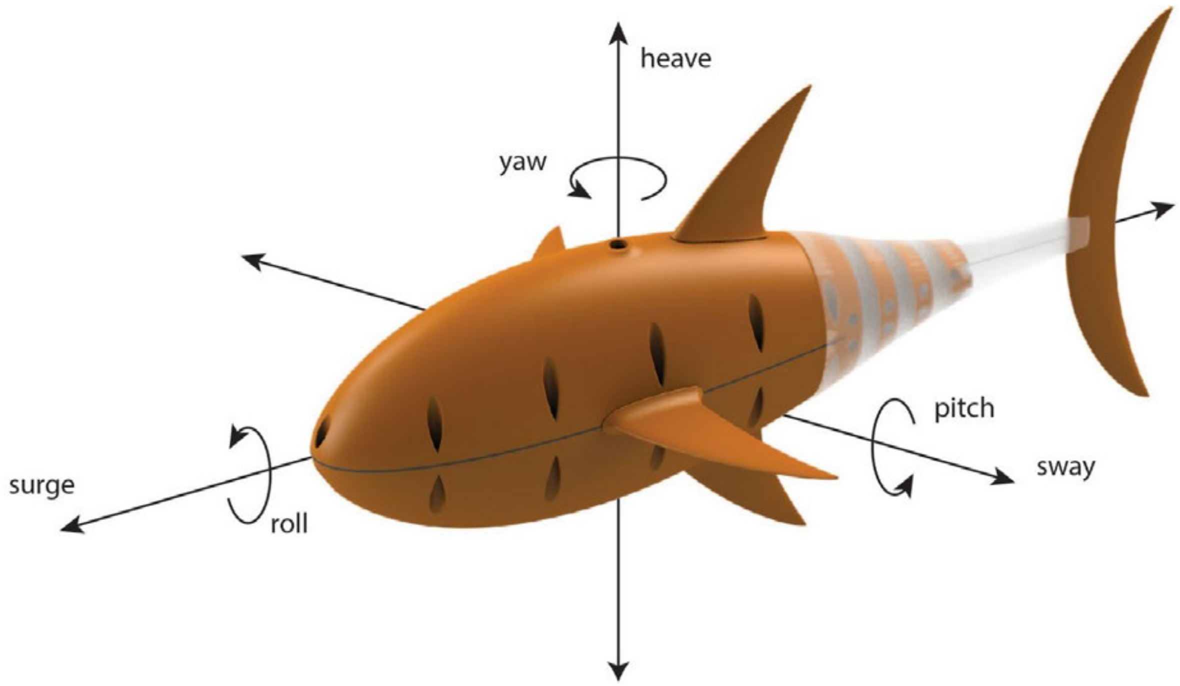

Figure 4.8: Definitions of robotic fish motions

When fish or robotic fish start to swim the oscillating tail motion can throw off its stability and it can start to move or rotate in an undesirable direction, most commonly sway and roll occur. Although the center of mass being below the center of buoyancy makes the fish less prone to roll and pitch. When it does rotate the displacement of the center of mass from below the center of rotation to a side during rotation is making it also sway a bit when it rolls and surge a bit when it would pitch. All these undesirable motions dissipate energy creating less forward thrust. To prevent these undesirable forces fish show adaptations we can learn from.

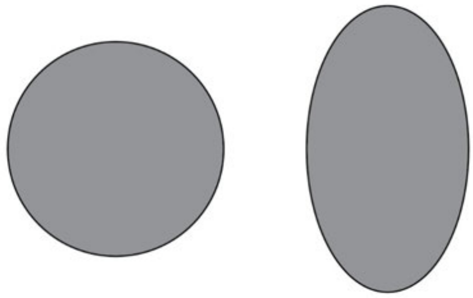

Figure 4.9: Frontal view of ideal hydrodynamic shape on the left and frontal view of a compressed elliptical body on the right

Compressed elliptical bodies Many fish species have developed vertically compressed elliptical bodies. Creating higher than width body ratio. This is not intuitive from a hydrodynamical point of view as minimizing drag around a given volume would result in a body of revolution. The clear advantage of this adaptation is the damping of the larger side surface area minimizing swaying motion during sideways oscillation of the tail (Lighthill, 1970[16]). But this shape also reduces rolling, the shape creates a larger distance between the center of rotation and dorsal and anal fins, preventing change in vertical angle (Weihs 2002[26]). This adaptation is absent in fish which need high maneuverability in both vertical and horizontal planes such as boxfish and dolphins.

Distribution of side surface area In fast swimming fish a large side surface area at a distance as far as possible from the center line of yaw rotation (defined by the line between the center of mass and buoyancy) is a common adaptation. You can witness this in body surface area such as with mahimahi and dorsal and anal fin placement of which a good example is the yellow fin tuna.

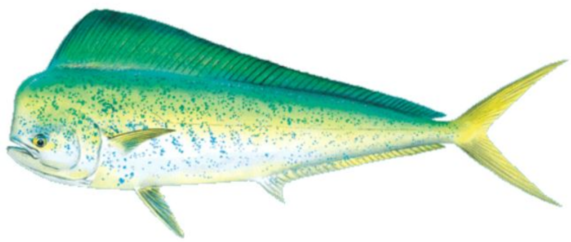

(a) A mahimahi, reproduced from Les Hata, Secretariat of the Pacific Community, https://www.hawaii-seafood.org/wild-hawaii-fish/mahimahi/.

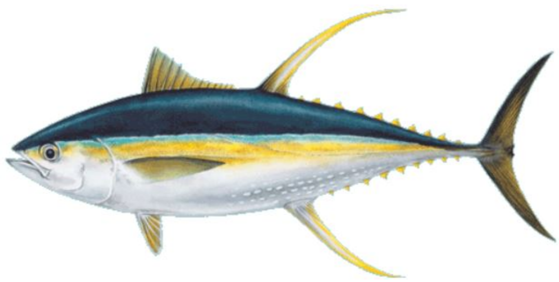

(b) A yellow fin tuna, reproduced from Les Hata, Secretariat of the Pacific Community, https://www.hawaii-seafood.org/wild-hawaii-fish/yellowfin-tuna/.

Figure 4.10: Examples of distribution of side surface in the fast swimming pelagic swimmers tuna and mahihai showing thin tail connections and large anterior area.

With a simplified 2D model we can visualize that increasing the distance of a large surface area from the center of rotation can have a positive damping effect. Assuming a completely static line between the center of buoyancy and gravity we can compare the damping forces of the side surface area of the rigid head between prototype 1.0 and 2.0. These forces create a counter swaying effect stabilizing the robotic fish.

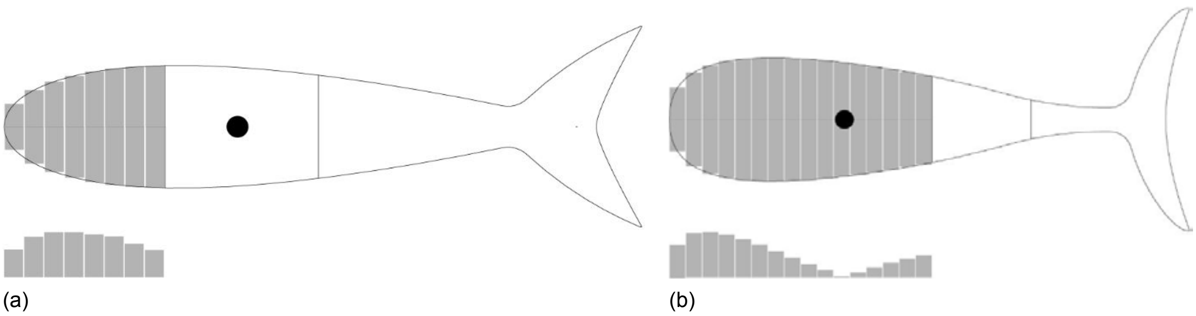

Figure 4.11: (a) Yaw damping force distribution on the rigid head of prototype V1.0. (b) The distribution of yaw damping forces on the rigid head in prototype v2.0. Below each figure a diagram shows the distance from the center of rotation (the black dot) times the surface area. Allowing to compare yaw damping taking into account the moment of inertia.

.

As the moment from the center of rotation increases the damping force increases. For maximum damping ideally you want as much side surface area to the front. However there will be trade-off with hydrodynamic forces which could favour a more streamlined side shape.

Dorsal and anal fins Stabilizing fins are most effective at the largest distance from the center of mass due to the increased moment. Therefore in general the largest fins are on top due to the center of mass on a submerged object being per definition in the bottom half.

5

Explorative experiments

5.1. Experiment #1: Numerical reproduction of fish swimming by an active/compliant robotic mechanism

5.1.1. Goal & method

To investigate if our compliant and active body system in a robotic fish could recreate thunniform swimming we take a look at reference footage of a swimming fish and try to recreate this exact motion with a numerical model made in Simulink Simscape based on an active tail segment and compliant tail segment. Parameters such as spring stiffness and damping of the compliant body were manually adjusted to investigate if similar movement could be reproduced with a compliant/active body mechanism. Sadly we were unable to obtain thunniform swimming reference footage, therefore mahimahi, another fast swimming pelagic swimmer was used as a reference.

5.1.2. Results

Video analyses from the mahimahi swimming footage showed the body moves along a sine wave pattern of ¾ wavelength and the tail is close to linear with the direction of travel, corresponding with the high efficiency results with pitching and heaving foils.

In the first panel in the figure below it can be seen that the angle at the highest heave amplitude of the sweeping tail motion can be 0 degrees, creating no thrust in the opposite direction of swimming motion. No problems were found in recreating the motion. The most important factors for recreation turned out to be the ratio compliant/active tail and stiffness of the compliant tail.

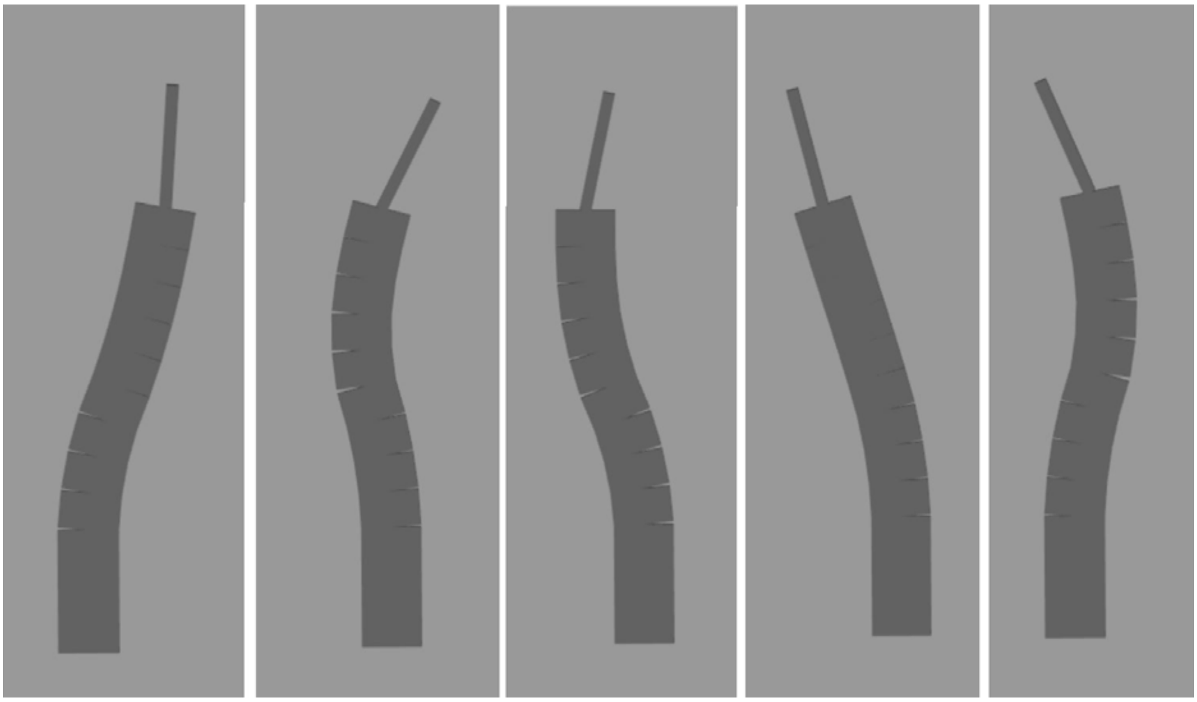

Figure 5.1: Screenshots of a simulated swimming machine comprising of a rigid non moving head, active sweeping body and spring damping body and tail.

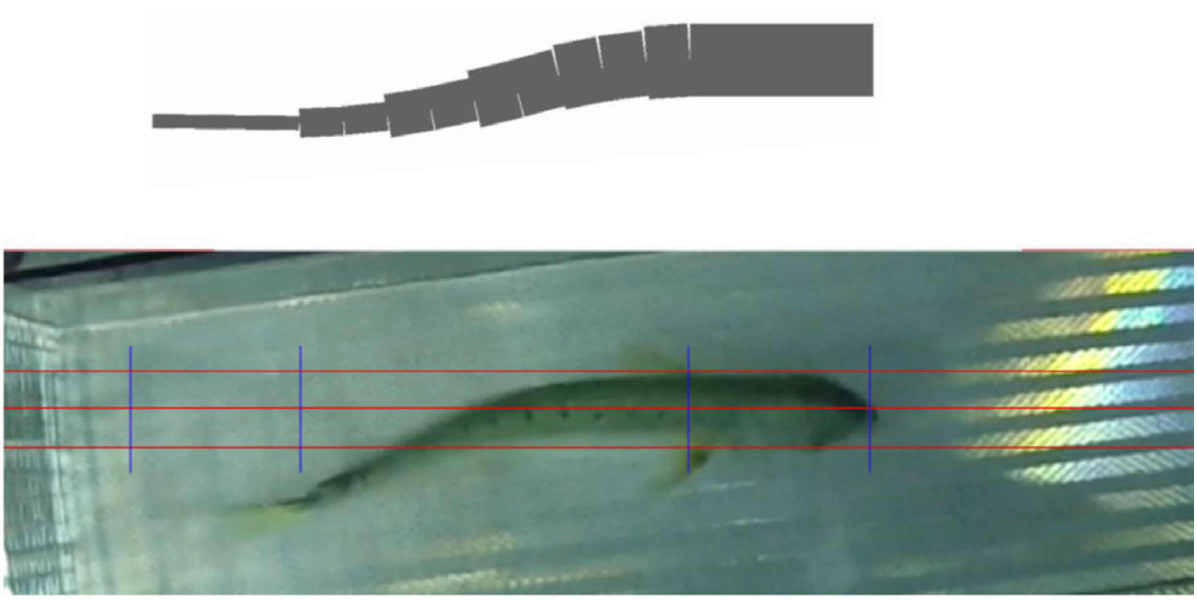

Figure 5.2: Side by side simulation and stabilized segmented reference footage of a mahimahi. Full video: https://youtu.be/LoBrGViYz6o

5.1.3. Conclusion & discussion

Based on analyzing the video footage of the mahimahi the swimming characteristics can not be described as thunniform. Lateral bending occurs through a large portion of the fish. This ratio between active tail and rigid head matches the characteristics of a carangiform swimmer (y Alvarado et al. 2003[28]). As reference footage from a real tuna turned out to be impossible to obtain (even though it is out there) our conclusions are based on a not completely comparable example to the robotic fish that is envisioned. This model is however easily adjustable to other reference footage if we would be able to receive such later on. Due to this footage not being thunniform it does not give insight in the ratio compliant, active tail and passive head for our thunniform swimming robotic fish. This will require us to build a more design iterations to find the right ratio for thunniform swimming. This model does show the influence of ratios and has shown precise oscillating motion can be accurately mimicked in a compliant/active segmented model.

5.2. Experiment #2: Swimming test mahimahi prototype

5.2.1. Goal

To create a starting point for the development of a robotic fish. This starting point is based on reference footage of a mahimahi. As a mahimahi swims, the assumption is this basic first prototype will swim as well as long as it mimics the motion reasonable. From that point variables such as tail stiffness and body segment ratios are expected to be adjusted to make it more efficient and fast.

5.2.2. Method

Based on video analysis of a mahimahi swimming in a laminar flow tank, first a numerical model was created consisting of an active and compliant tail part. Based on the ratio of tail, compliant body, active body and rigid head a prototype was designed with the same characteristics enabling to mimic the motion of the mahimahi closely.

The prototype consists of a 3d-printed rigid head housing a single servo and in the future possible other electronics. The active body consisting of a flexible polyester backbone and 3d-printed ribs creating the outer contour. The last rib near the tail is pulled by cables to create an arc. The compliant body extends this curve into an sinuid motion. The caudal fin sweeps. The body was water sealed using a latex laboratory glove and stretchable tape. This method although not ideal enabled a quick prototyping and validation.

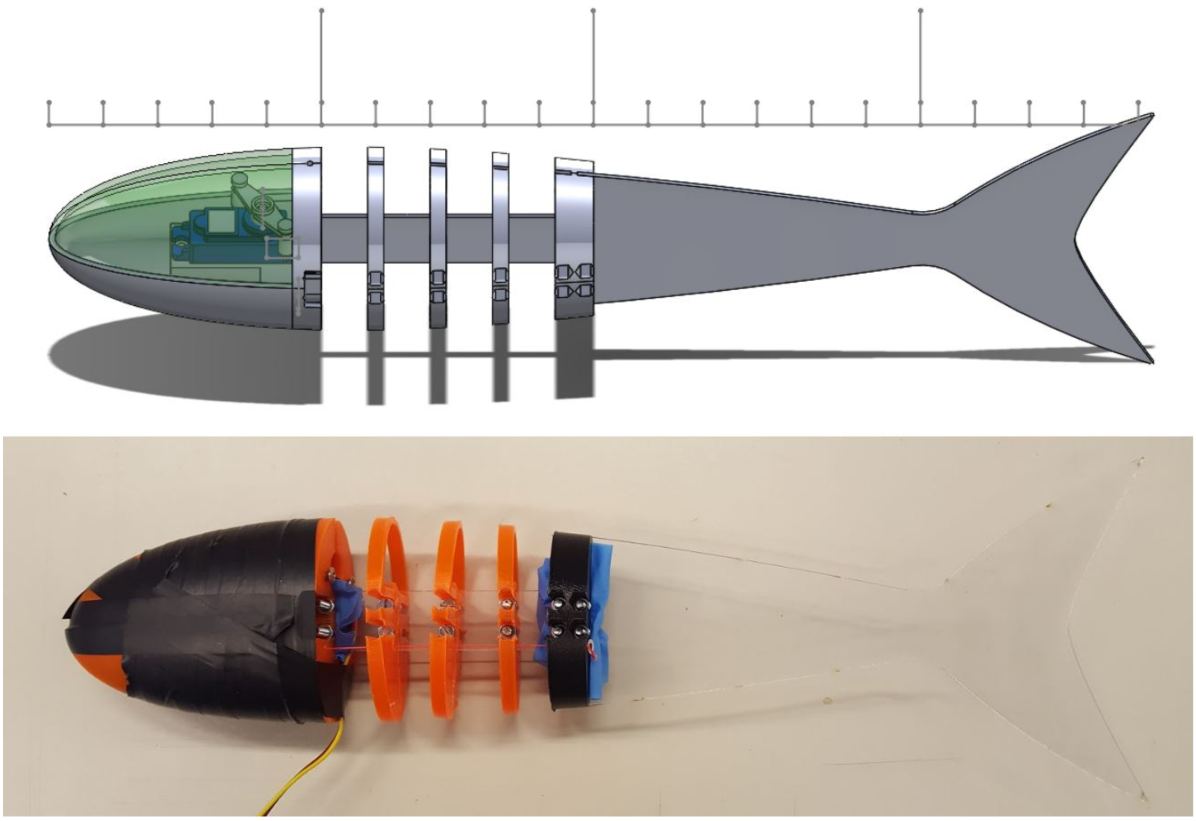

Figure 5.3: 3D-model design and prototype with the same body ratios as the mahimahi from the reference footage.

5.2.3. Results

Barely any forward movement can be observed. There is a strong side to side swaying of the head, some rolling as well.

Figure 5.4: Still frame from video showcasing the minimal forward movement of the first prototype. Video: https://youtu.be/0RJSgPRmzJk.

5.2.4. Conclusion & discussion

The prototype is clearly producing very little thrust. Further literature research shows that some fast swimming pelagic swimmers like sailfish and marlin, are inherently very unstable due to their high flexibility (hebrank et al. 1990[9]). They therefore actively use their fins and head to counter instability and to stay on course (S. marras et al. 2015[18]). This would explain some of the behaviour we are seeing from the prototype. From this we can also conclude that the mahimahi footage was inadequate as a reference. Further research into the stability is executed in the chapter stability to better understand why this prototype was unstable and how to resolve this.

5.3. Experiment #3: Numerical analyses of yaw stability

Increased yaw stability increases the tailsweep amplitude and therefore speed and efficiency. We investigate 2 common body shapes in stable fast swimming fish on their influence on yaw stability. We further isolate the identified characteristics of these body shapes in experiment 3.3 and 3.4. Producing better understanding which characteristics and to what extent they can be attributed to positive yaw stability.

5.3.1. Experiment #3.1: Investigating yaw stability effects of increasing rigid head length

Tuna show a very large rigid head to thrust inducing tail ratio. The ratio between this thrust inducing tail and passive head has a very high influence on the yaw stability. When the distance between undesired yaw force originating from the caudal fin, and the center of rotation increases it will yaw less. The force to accelerate and decelerate the body rotationally increases with distance (moment of inertia). This effect due to increased moment of inertia also works positively on the damping effect of the anterior portion of the fish.

In this experiment we investigate the effects of moving the center of mass forward and increasing mass by extending the rigid head. Increasing the length of the head, decreases the mass ratio between the angular force inducing tail and passive head, the tendency to resist angular acceleration should increase. Increasing the length also increases damping due the interaction of the side surface area with the surrounding water. This will however not be taken into account in this experiment.

Method We show the influence of the change of moment of inertia on head swaying amplitude and tail amplitude with a model. Only the effects due to the change of position of the center of rotation/mass and mass distribution along the body are taken into account. We increase the length of the passive head placing the center of rotation at ⅖, ½ and ¾ and compare the effects on yaw stability.

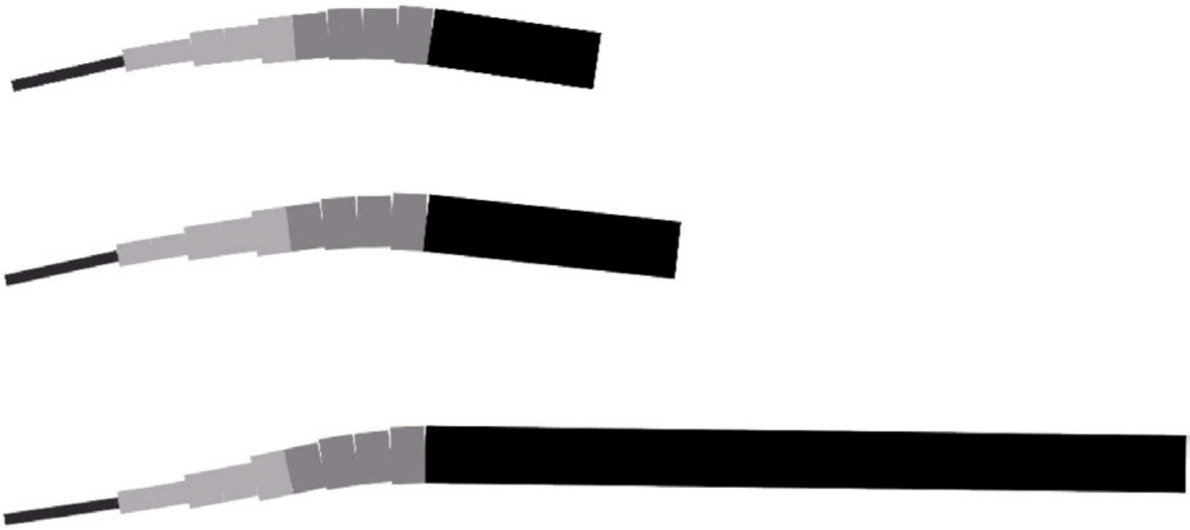

Figure 5.5: The center of rotation is placed at the center of mass of the complete body the rigid head is ⅖, ½ and ¾ of mass of the total body. Black on the right is the passive head, dark grey active tail, light grey passive tail, black on the left, the caudal fin. Screenshot is taken at the maximum tail amplitude. Video: https://youtu.be/oxUJU0yoq6w

Conclusion Increasing head length in relation to the actuated tail when width and height stay the same has a positive effect on yaw stability. This can be clearly concluded from figure 5.3.

5.3.2. Experiment #3.2: Investigating yaw stability effects of redistributing mass to the anterior by increasing head height

A common adaptation in nature instead of increasing the rigid head length is changing the volume/weight distribution such that the tail connection is slim and the front of the head is high. This can for instance be witnessed in sailfish, mahimahi and marlin.

This has not only positive effects due to the surface area interacting with the surrounding water as mentioned earlier, but also due to moving the center of rotation forward just like increasing the rigid head length. In this experiment we investigate the influence of redistributing mass further forward towards the head by increasing the height of the head.

Method We show the influence of sway by comparing 2 simulations. One with the center of rotation at the attach point of the rigid head, and one with redistributed mass by increasing the head height moving the center of rotation from the attach point of the rigid head to ⅓ of the rigid head.

Figure 5.6: Overlay of 2 models, one having a weight distribution placing the center of rotation at the connection between the rigid head and first rib. 2nd having the weight redistributed to move the center of rotation to ⅓ of the rigid head. Black on the right is the passive head, dark grey active tail, light grey passive tail, black on the left, the caudal fin. Video: https://youtu.be/4-2$_5kffDck$

Conclusion & discussion The yaw stabilizing effect of redistributing mass to the anterior portion is positive. Both adaptations in experiment 3.1 and 3.2 are clearly beneficial for stability. To what extend and due to which properties can not be concluded without isolation experiments. The effects of redistributing mass to the anterior can not be compared to increasing the length of rigid head without controlling for mass.

5.3.3. Experiment #3.3: Isolating the effects on yaw stability of the displacement of the center of rotation

We investigate the effects of displacement of the center of rotation by controlling for mass.The damping effect on the anterior portion of the head will increase as well due to the increased moment arm when the head is extended.

Method We show the influence of displacing the center of rotation on yaw rotation by comparing 2 simulations. One simulation has double the rigid head length as the other. Both have the center of rotation at ⅓ of the total head length. The total mass is the same. This is controlled for by reducing the head height of the longer head.

Figure 5.7: Comparison of yaw stability by redistribution of mass by increasing head height and head length. Both simulations have the same total mass. The center of rotation is with both the same fraction of ⅓ of the rigid head, increasing the distance between the center or rotation and the actuated tail in the long head simulation.

Conclusion The displacement of the center of mass forward shows an increase in stability. This can be attributed to the center of rotation moving further forward, increasing the moment arm between actuator and center of rotation. Also the extended moment arm between the mass at the anterior of the head will induce more damping.

5.3.4. Experiment #3.4: Isolating the effects of mass

We isolate the effects of mass from the displacement of the center of rotation at the same distance from the actuator by variating the head length.

Method 2 simulations are compared based on their influence on yaw stability. The center of rotation is kept at the same distance of ⅓ of the short head. To keep the distance of the actuator to the center of rotation the same, the total mass of the long rigid head is half of the shorter head with mass ratios between the tail and short and long head of ¾ and ⅘ respectively.

Figure 5.8: Comparison of yaw stability with different head length and the center of rotation at the same distance from the actuator.

Conclusion & discussion the increase of mass of the rigid head has a positive influence on yaw stability. The damping due to the increased distance between the center of rotation and the anterior portion can not compensate for this decrease of mass. Concluding that increased volume/mass outweighs the dampening of the anterior portion when center of rotation is at the same distance from the actuator. This does not take into account dampening due to the surrounding water which may make the longer head configuration come ahead as the difference is fairly small.

5.3.5. General conclusion

We have investigated 2 common adaptations in nature, a long rigid head such as common in tuna and a high distribution of mass to the anterior of the fish. We isolated the characteristics of these adaptations to further investigate their influence. We identified 3 aspects which positively influences yaw stability in these experiments: increased length between center of rotation and actuator, increased anterior mass/volume ratio and increased moment arm between the damping anterior and center of rotation.

When the center of rotation is within the rigid head, the distance between the center of rotation and force inducing tail will be increased to a lesser extent by increasing the head height than by increasing the length of the head. When length is of no concern, as shown in experiment 3.4, it would therefore be most beneficial to increase head length increasing the distance from the actuator to the center of rotation as much as possible. When length is a limiting design parameter it can be beneficial to increase the mass ratio to the anterior instead. Both can also be combined to generate more stability if needed.

5.3.6. General Discussion

These experiments do not taken into account the damping due to side surface area, and negative speed influence of increasing frontal area by increasing the height. Frontal area will not increase with length making increasing length even more beneficial.

There is a balance at play with an optimum dependent on the specific requirements of a (robotic) fish. In an assumed completely straight forward moving rigid head the as large as possible actuated tail creating a high tail sweep amplitude has shown to be most efficient (chapter 4.3. Body kinematics for fast efficient swimming). This is due to the ideal angle of the caudal fin is maintained over a longer distance. The vortices created at the tip of the motion which create losses are also a smaller portion of the complete thrust inducing moment.

However the rigid head will never move in a complete straight line. There will always be some yawing, and that yaw is loss of energy. As can be seen in the above model the yawing increased when the ratio between the tail and head increases. These two parameters of efficiency work in complete opposite direction. Not taking into consideration other factors there would be a single point optimum. However a lot more forces and desired characteristics are at play such as maneuverability. As the sideways stability increases, maneuverability in the same direction decreases. Resulting in a possible undesirable large turning cycle.

5.4. Experiment #5: Experimental validation of stabilization

The theory and numerical models explain why the prototype v1.0 showed significant stability issues and almost no forward thrust. One of the main reasons was that the first prototype had its center of rotation to far backward even within the actuated tail part. The object wants to move around its center of mass creating a motion of the head and tail yaw in the same direction. There is also very minimal side surface area on the anterior part of the fish countering the head swaying. We moved the centerline of rotation further forward into the passive head by extending the passive head with an extension piece to counter both issues.

5.4.1. Results

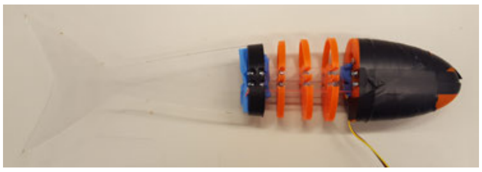	
Prototype v1.0 **Design** Based on the motion of a mahimahi in a laminar flow tank.	**Prototype v1.1** **Design** An extension piece is placed between the head and compliant body to move the center of buoyancy (and center of mass) from the active tail into the passive head. The extension piece also somewhat increased the surface area to the anterior portion of the body.
Observation Barely any forward moving, significant swaying of the head, minimal actuation of the compliant tail.	**Observation** Clear improved forward motion and stability. Still some significant head sway.
Video prototype v1.0 https://photos.app.goo.gl/Mu74u32nSBRAmUbL7	**Video prototype v1.1** https://photos.app.goo.gl/MXmbz8KZHmnK3zvH9

5.4.2. Conclusion

The experiment confirms in line with expectations based on the models and theory that increasing the length of the rigid head placing the center of mass outside of the active body into the passive head increases stability and forward thrust significantly. Therefore confirming this was the origin for the poor performance of prototype v1.0.

5.4.3. Discussion

The increased anterior surface area reduced head swaying. There is still some roll. As explained in sub chapter 4.6.2 Yaw and roll stability, this can be countered by creating a more elliptical body. This could also increase yaw stability further by improving anterior side surface area while keeping the center of rotation at the same distance from the anterior.

5.5. Experiment #6: Experimental validation of stabilization features

Based on the conclusions of experiment 2 till 5 a completely new prototype is built. The following improvements have been implemented:

- Increasing side surface by increasing the anterior height
- redistributing mass to the anterior by increasing head height and reducing tail height.
- The caudal fin height is increased and chord length reduced, reducing loss in vortex creation on the tip of the fin Increasing efficiency.
- Overall build quality of both body and 3d-printed ribs are improved.

5.5.1. Method

We compared the swimming properties of both prototypes based on stability and forward thrust. Both prototypes swam a short stretch in a water tank based on which observations are made.

5.5.2. Results

	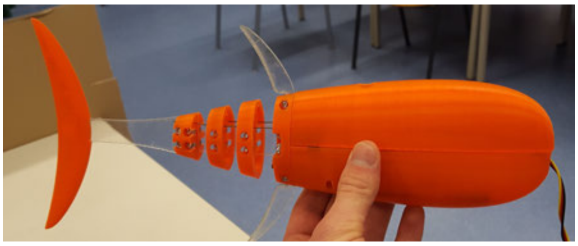
Prototype v1.1 **Design** An extension piece is placed between the head and compliant body to move the center of buoyancy (and center of mass) from the active tail into the passive head. The extension piece also somewhat increased the surface area to the anterior portion of the body.	**Prototype v2.1** **Design** A complete redesign showing a redistribution of mass and volume to the anterior part of the robotic fish. Increased caudal fin height and reduced chord length reducing loss in vortex creation on the tip of the fin Increasing efficiency.
Observation some head sway and roll instability. stable forward motion.	**Observation** Sufficiently stable in all directions for continuous forward swimming. Clear increased speed. Still some minor head sway and minimal roll is observed. Measured top speed 389.6 mm/s 1.2 body length/s
Video prototype v1.1 https://photos.app.goo.gl/MXmbz8KZHmnK3zvH9	**Videos prototype v2.0** video 1: https://drive.google.com/file/d/19Do8ThaceUOSyeKsSUkj-gE6n4kTOO71/view?usp=sharing Video 2: https://drive.google.com/file/d/1KH8v6JoqWDnpob82C6jTg-OX-eHRSOfB/view?usp=sharing

5.5.3. Conclusion & discussion

In prototype v2.0. still some minor side swaying and some minimal roll was observed. This could be countered by adding dorsal anal fins and pectoral fins respectively.

To save time multiple modifications (caudal fin design and body shape) have been implemented in this model. Making it impossible to deduce if the increased performance is due to one or the other modification and to what extend. Based on the theory and numerical simulations we were confident that all adaptations would increase performance and therefore this experiment was less about quantifying improvement but rather making big steps as fast as possible to eventually end up with a prototype which can be fine tuned based on more quantitative results.

5.6. Experiment #7: Comparison of rigid caudal fin with flexible mackerel fin

5.6.1. Goal

A small experiment was set-up to verify the theory that a soft tail could potentially create higher thrust and to what extend. The purpose of this experiment is to give a rough estimate of the influence flexibility of the caudal fin on speed. This is used to determine whether or not to pursue to include this design parameter in the final prototype.

5.6.2. Method

A fresh mackerel caudal fin was attached with superglue to our robotic fish prototype. If the tail would not have been fresh the fin rays in the caudal fin would not have bend properly into the direction of pressure. A mackerel tail was chosen as it is one of the few thunniform swimming fish which is widely available and of similar size as the prototype. With this tail a high tailbeat frequency straight swimming path was recorded and compared to a 3D-printed reference tail.

5.6.3. Results

The mackerel tail creates a much more soft and fluent motion. This is most likely due to the damping effect of a flexible caudal fin.

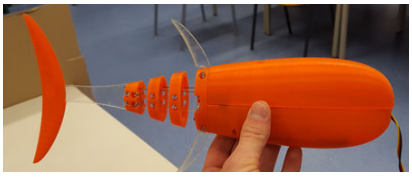

Caudal fin surface area	2430.93mm^2	1304.743mm^2
Top speed mm/s	389.6	305.0
Top speed bodylenght/s	1.2	1.0
Videos	https://drive.google.com/file/d/19Do8ThaceUOSyeKsSUkj-gE6n4kTOO71/view?usp=sharing	https://drive.google.com/file/d/1Lxs4d-9k4JzVuFHh$_v3C6nplz8d8LaIY/view?usp = sharing$

5.6.4. Conclusion

It is difficult to deduce exact conclusions from these results. To quantify the effects of a compliant tail we simplify the forces by assuming the increased displacement of water is linear with the surface area of the caudal fin. Therefore the forward thrust force (F_t) increases linearly with the surface area of the caudal fin. The hydrodynamic drag is the only force to overcome. Hydrodynamic drag is commonly expressed as:

$$F_D = (1/2)\rho S v^2 C_D$$

Where ρ is density of the fluid, v, speed, S, reference area and C_D the respective drag coefficient. Only the speed changes. The resistance of the surrounding water increases quadratically with a linear increase of the speed. The thrust force (F_t) and drag forces are in equilibrium when swimming at a constant speed. There is a power law relation between:

$$F_t = F_D$$

Where with the same body and in the same fluid

$$F_{\mathrm{D}} = v^2 x$$

F_t increases linearly with surface area of the caudal fin. X is a constant value which replaces all non changing values. Filling in the values of the prototype with the lunate 3d-printed tail leaves us with an x constant value of 0.016. Based on the quadratic increase of drag, if only the tail surface area was decreased the smaller real tail should have gone 285.4mm/s. The measured 305.0mm/s is a 7% increase in speed.

5.6.5. Discussion

It is impossible for everything to stay exactly the same. Frontal area may have changed very slightly due to the placement of stabilizing leads. The shape of the tail is different. The center of both caudal fins may not be placed at a perfectly similar distance. If the caudal fin is placed further to the back this would increase the amplitude of the tail sweep. The results could also have been better with a perfectly tuned caudal fin flexibility for the tested speed. The speed for which the flexibility of our tail is tuned was unknown.

Taken all unaccounted variables into account we can not conclude a 7% increase can be attributed solely to the flexibility. However it is by far the biggest difference in both experiment and the most likely cause of the increase.

Implementation of flexibility in line with theory and advice from experts could be beneficial for speed performance. Due to the limited time and expected higher increase of speed due to increased frequency this adaptation may not be implemented in the final prototype however.

6 Final high frequency prototype

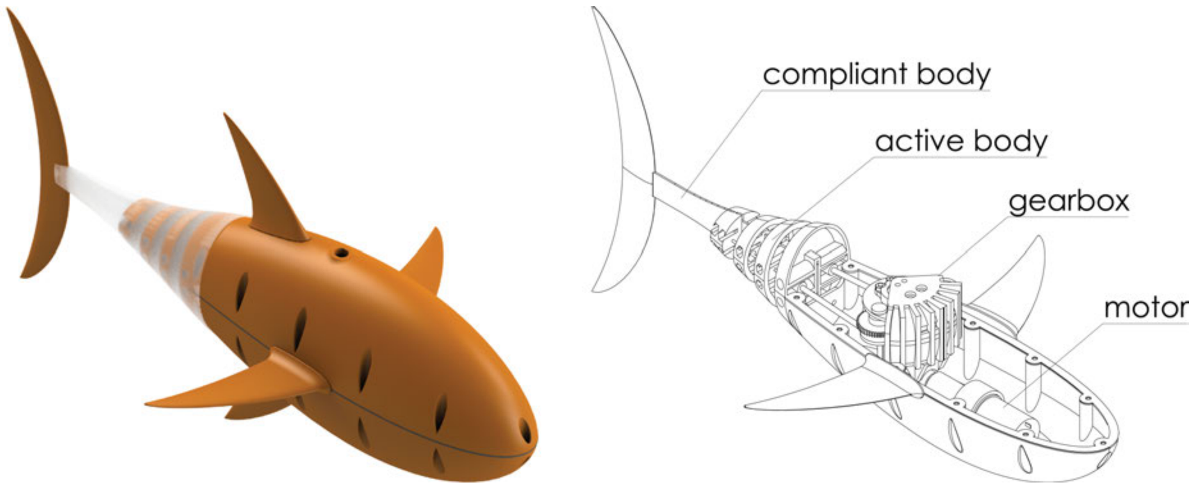

Figure 6.1: Final prototype rendering and drawing with most important components indicated

.

A servo driven prototype is not able to maintain frequencies above 3 Hz. To increase the frequency of tail sweeping we have to change the design to use a common rotary DC motor. This chapter showcases the redesign of the robotic fish enabling to implement a rotary motor, taking into account all we have learned from previous chapters.

6.1. gearbox

The basic design consists of a DC motor and 2 gears on opposite sides of the motor shaft rotating in opposite directions, pulling on the left and right side in a half cycle delay from each other. Such a DC motor driven active body does not only allow for higher frequency but also allows for a cosine wave motion of the active body. This enables a more fluent cosine wave motion for the caudal fin. With a servo driven design the rapid change of direction creates a more sawtooth heave motion. The short stop before changing direction might even create a trapezoid motion. At a maximum angle of attack of 20° and strouhal number of 0.3 Hover (F. S. Hover et al. 2004[10]) has shown that both a sawtooth and square angle of attack profiles are approximately 20% less efficient than a cosine profile. Indicating a more continuous motion, which the DC motor provides positively influences the efficiency performance of the oscillating system.

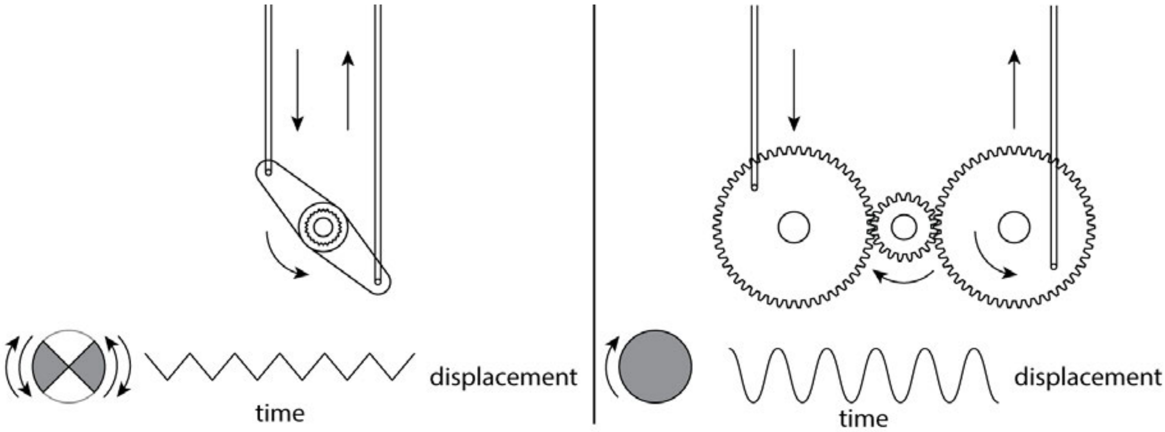

Figure 6.2: On the left a servo driven design, on the right the basic principle of the DC motor driven design. A graph of vertical displacement of the wires over time is depicted underneath both illustrations.

	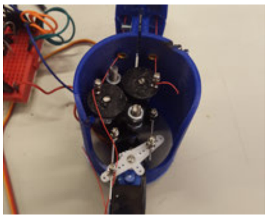	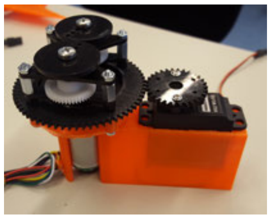	
	Changes Anchoring does not put pressure on the gears or shaft anymore.	**Changes** Size of the system is increased to enable better anchoring. Ball Bearings are introduced to turn more smoothly.	**Changes** A right angle gearbox is used to reduce the height of the system allowing very large motors to be implemented if needed. An extra overhang is used with ribs to increase stiffness and decrease movement of the gearbox at high rotations.
Results Barely ran, too much play when bolts are not tightened enough. Does not turn when bolts are tightened.	**Results** Significant undesired movement within the gearbox. Needs more anchoring.	**Results** Steering system works successfully. No undesired vibrations. Stable and fluent motion of the gearbox. The four anchoring point on the outside of the gearbox make it too large.	**Results** Gearbox runs very smooth.
	Test footage https://photos.app.goo.gl/jMmETB7Pzo9wvfwj7	**Test footage** https://photos.app.goo.gl/6wyxSd9m4iJsKMDs8 https://photos.app.goo.gl/gbqEwaeQJhnH9RDm9	**Remarks** At the top there is a space to add the steering system tested in previous prototypes. It was decided to remove this out of this prototype to reduce variables for straight forward testing.

Table 6.1: Progression of gearbox prototypes

6.2. Shape

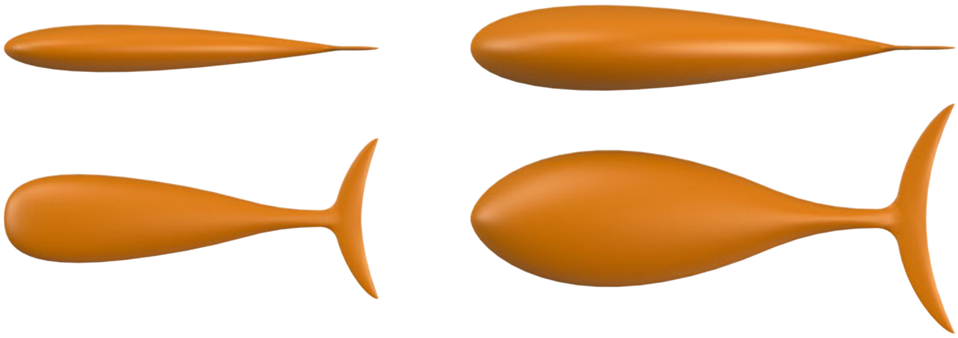

Figure 6.3: Comparison between shapes of previous servo driven prototype and DC motor driven prototype. There is a clear increase in width due to gearbox.

The width of the body was increased to accommodate the gearbox and motor. To keep a hydrodynamic shape the length increased as well. Due to the increased length of the rigid head, which has a stabilizing effect and the increase of frontal area which increases hydrodynamic drag, a more pointy thunniform head shape was chosen. Which would create less sway resistance but is more hydrodynamic.

6.3. Motor controller & wireless communication (discontinued)

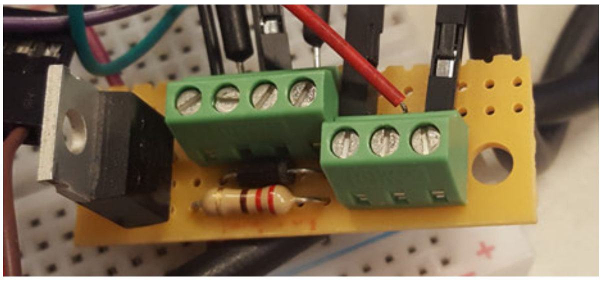

Figure 6.4: Motor controller used during testing.

A motor controller and wireless communication unit was designed for this prototype which at the end was not implemented. The motor controller could not supply enough current at low voltages for the motor to turn slowly. After discussions with powertrain engineers I decided to use an external power supply to power the fish for better speed control during testing. It is possible to design a motor controller able to create the required 1.5 ampere at low voltages, however to save time and to keep our eyes focused on the goal of high efficient fast swimming it was decided to opt-out on further improving the motor controller design.

When the motor controller was discontinued the wireless communication was discontinued as well even though it worked quite well (tested only at low depths up till 20cm). Wireless communication would only have a purpose if the design was completely wireless.

Some of the arduino code can be found in appendices A, B and C.

7

Validative experiments

7.1. Experiment #8: Influence of frequency on speed

7.1.1. Goal

From previous research in fish by Bainbridge[4] and the robotic validation by Clapham[5], we can already conclude that increasing tail beat frequency will increase speed. This of course assuming all variables remain the same. After creating a stable swimming prototype a prototype enabling high tail beat frequency was built. In this experiment we tested this prototype, tried to reach peak performance, and analyse what happens at peak performance disallowing it to go faster/more efficient.

7.1.2. Hypotheses

- Speed should increase with frequency.
- A drop off should occur at a certain frequency. When the frequency is too high for the compliant tail it will first start to overbend past the ideal angle of attack of 20.2 degrees. Eventually it will bend to such an extent, the amplitude of the caudal fin will decrease and come close to stalling.

7.1.3. Method

The prototype is fitted with a stiff compliant tail to accommodate the desired bending of 20.2 degrees max. occurs at a high tail beat frequency. A camera is placed parallel above a bath of water. Camera (GoPro7) is set to linear settings to minimize deformation due to the lens and 1080p, 120 fps. Aligning the fish perfectly parallel to the water and camera is difficult therefore calculations illustrated in fig. 7.1 are used to compensate for misalignment and accurate determination of traveled distance speed.

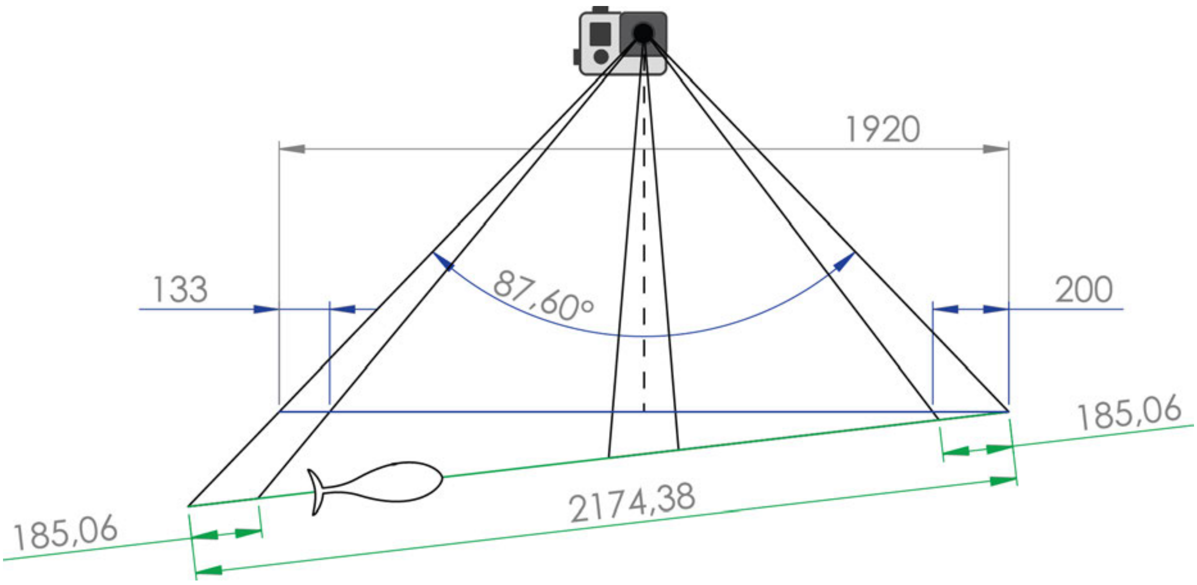

Figure 7.1: The camera lens makes a horizontal angle of 87,6 degrees[1]. In this example a segment of the fish with a known length 0.2481m is 133px at the beginning of the measurement and 200px at the end of the measurement. Taking into account the projection the known segment of 0.2481m is 185.06px and has traveled a total of 2174,38px within the frame.

We measure the speed by using the average length of a known segment of the fish to calculate the distance traveled divided by the time. We measure the speed from the lowest voltage the motor starts turning, which is 5v. The voltage is increased by increments of 0.5v till failure of the prototype or the maximum specification of the motor are reached. At each voltage the experiment is redone until we captured at least 3 good straight swimming samples. To calculate the strouhal number the tail amplitude is measured when the robotic fish is in the middle of the camera view to minimize any field of view deformation. The length of the tail sweep amplitude is compared to the reference length onscreen of which the real length is known.

7.1.4. Results

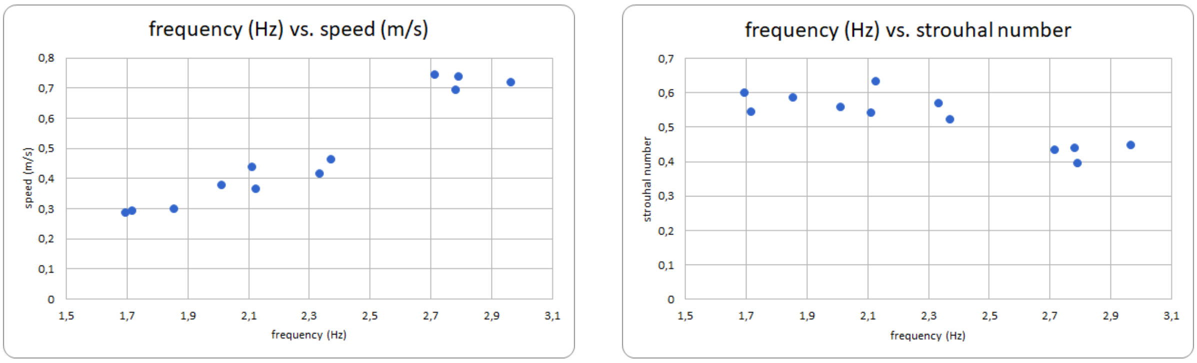

(a) (b)

Figure 7.2: (a) Relation between tail beat frequency and speed. (b) Relation between tail beat frequency and strouhal number, indicator of efficiency.

(a) (b)

Figure 7.3: (a) Large angle to the direction of swimming at the top of the heave amplitude at 2.3 Hz (9v). Showcasing little deformation of the compliant tail. (b) at top heave amplitude.S shape deformation starts to occur. Image at 3.0 Hz (11.5v).

Due to problems with the backbone and motor we have not been able to increase frequencies past 3 Hz. The deformation of the compliant tail start to lightly occur at around 2.7 Hz (9.5V) at lower frequencies the minimal deformation of the compliant tail makes the tail pass far above 0 degrees from the direction of swimming at the top of the heave amplitude actively creating thrust in the opposite direction slowing it down. The strouhal numbers are between 0.39 and 0.59. This is on the high side for optimum efficiency, which occurs at a strouhal number between 0.2 and 0.4. Exact values can be found in appendix D.

7.1.5. Conclusion

A clear trend can be seen between speed and frequency. From the high strouhal optimum we can conclude that for the size of the stroke amplitude, speed, frequency relation a higher frequency would be more efficient. By analyzing the footage closer we can see the compliant tail does not make the desired S-shape, further adding that frequency should be increased or stiffness of the compliant tail reduced for optimal performance.

7.1.6. Discussion

The testing has been done over many days due to parts failing including, communication failure, cable breaking, waterproofing failing, motors blowing up,flexible backbone in the active body shattering at high frequencies and sadly many many more issues. Due to these issues there is some inconsistency between test days. Although consistency was thrived for, a slightly tighter screwed backbone, a lead for adjusting the center of gravity at another place can all have small influences on the performance. However a general trend can still be deduced from these results.

The measurement of speed is based on a reference body length. It turned out to be very difficult to let the robotic fish go in a way that made it swim completely parallel to the water surface. It often slightly dove or rose. This was compensated for in our method of deducing speed however it can be assumed this aspect increased our error margin. In general we can conclude that very precise speed data is very hard to record in a completely free swimming robot without more complex measuring equipment.

7.1.7. Recommendations

Some recommendations are easy to incorporate, others are more hypothetical as for our testing it would take too much time to incorporate. An easy to incorporate modification is to change the material of the backbone in the active tail segment. When testing is done for an extended time or at high frequencies the PETG backbone cracks. Most likely due to fatigue and a too low flexural modulus.

If testing is done for such an extended time it is also advised to switch the material from the 3D printed head from PLA to a more durable material such as ABS. The body has started to crack around the screws which connects the two halves. This modification will most likely not be incorporated in the next version due to time constraints. The 3D-printing in a more durable material brings extra issues with it such as warping when cooling down. To get this done well will take more time than reprinting parts in PLA.

Reducing head sway might further improve performance and ease of testing. Testing with pectoral, dorsal and anal finds could result in a faster more efficient swimming fish. More validation is needed for this conclusion.

7.2. Redesign: New backbone

Testing could not continue due to the repeated breaking of the flexible backbone used in the active tail. The PETG material used was previously chosen based on its flexibility and availability. The PETG sheet brakes when high flexural strain is repeatedly applied and removed at high frequencies. It could be concluded that the material was not tough enough. We want to maintain the same or slightly lower flexural modulus as the backbone needs to be able to bend easily but also be stiff enough to support the ribs and not collapse under the pulling forces applied by the wires. The PETG sheet could bend repeatedly to the same angle at lower frequencies without plastic deformation. Concluding yield strength was sufficient. Based on these experiences with the PETG the following requirements where set-up.

Core requirements

- **Toughness > 4 kJ/m^2**, for less brittleness, more ductile (like rubber) than PETG
- **Flexural modulus range range of 1 to 2 GPa**, (similar to young's modulus) how easy it bends, similar or slightly lower than PETG
- **Yield strength >48 MPa**, the elastic limit at which plastic deformation starts to occur

Extra

- **Fatigue strength > 26 MPa**, can withstand higher cyclic stress

Table 7.1: Backbone material comparison

	Toughness (kJ/m^2)	Flexural modulus (GPa)	Yield strength (MPa)	Fatigue strength (MPa)
PETG	2.18-3.1	2.01-2.11	47.7-52.9	24-26
PA12 (rigid)	8.01-10.7	1.17-2.01	34.4-43	19-21

using CES EduPack 2018, PA12 was selected out of a total list of 70 materials meeting the core requirements for toughness and where within the flexural modulus range. PA12 is the only material in the list easily obtainable in small quantities in the desired 1mm thickness. The yield strength requirement was not met. However the minimum required yield strength is unknown thus the lower yield strength might still suffice. Fatigue strength is an indication of durability when cyclic stress is applied. Like in our experiment. Although a high fatigue strength is desirable for long levity it is most likely not the cause of earlier failure. This a slightly lower fatigue strength will impediment the material choice.

7.3. Experiment #9: Influence on stabilizing fins

Based on the literature study on stability adding pectoral and anal fins potentially increasing speed and efficiency performance. To investigate the influence of anal, dorsal and pectoral fins on speed and stability we executed the following test.

7.3.1. Hypotheses

It is expected that the dorsal and anal fin reduce yaw and the pectoral fins reduce pitch. This increased stability should aid in swimming in a straight line. The increased stability in yaw should increase the caudal fin sweep length, increasing speed. The increased frontal surface area and possible vortex creation at the fin tips will induce extra drag. It is expected that the increased caudal fin sweep length outweighs the small increase in surface area and possible vortex creation, thus increasing speed.

7.3.2. Method

The improved prototype (new backbone) was fitted with glued on pectoral, anal and dorsal fins. The anal and dorsal fins were placed as far to the back as possible. Still leaving space for the silicon skin to be taped in. The pectoral fins are placed in the middle of the axes of vertical rotation. The prototype was for a large part taped in to prevent leakage due to cracking of the PLA body. The speed was measured with the same method as in experiment #8. The results of the robotic fish with fins is compared to the results of the fish without fins of experiment 8.

7.3.3. Results

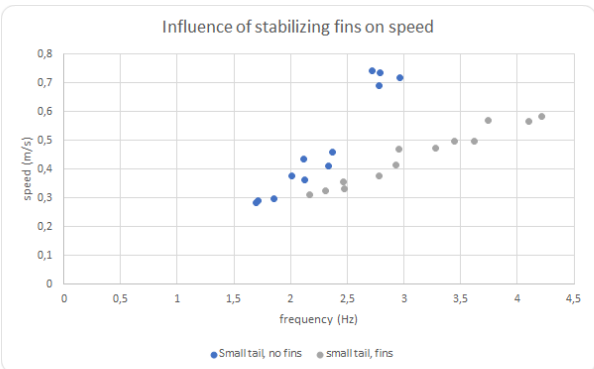

Figure 7.4: Comparison of speed performance due to added anal, dorsal and pectoral and reduced tail sweep amplitude of 11%.

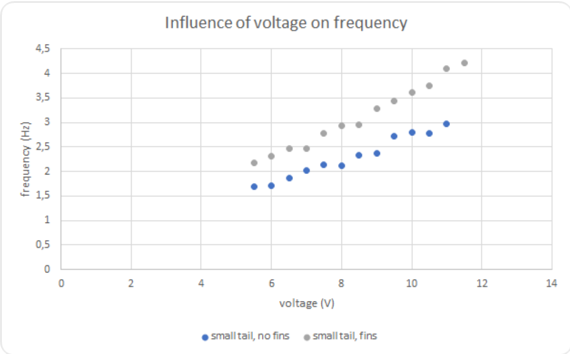

(a)

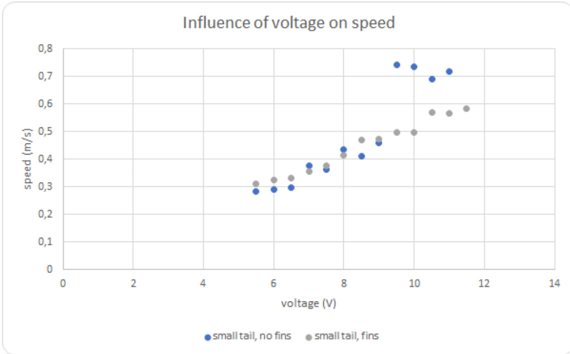

(b)

Figure 7.5: (a) Showcasing the small tail with fins had a significant increase of tail beat frequency for the same voltage input. Indicating the tensioning wire is loser in the tail with fins experiment which reduced the resistance, increasing frequency. (b) Graph showing the voltage input to speed relation.

There is a clear decrease in speed at the same frequencies with added stabilizing fins. Both pitch and yaw instabilities are reduced. Sweep length decreased from an average of 0.1m to 0.09m. Exact values can be found in appendix D.

7.3.4. Conclusion & discussion

The reduction of sweep length and as a direct result reduction of speed is not in line with expectations. This behaviour could be explained by a reduction of wire tension in the active tail between the test of the small tail without fins and the small tail with stabilizing fins test. The wire is a part of the prototype which is difficult to keep constant as even with tightening of screws it tightens a little bit more. This hypothesis can be verified by comparing the voltage used to control the speed of the robotic fish.

When supply voltage is constant, motor speed is inversely proportional to the load on the motor. Thus when the load was decreased due to the loser wires making the tail beat amplitude smaller the rotational frequency should increase proportionally (not taking into account increased resistance of the surrounding water). From graph 7.5a we can indeed conclude the frequency increased with the same voltage input. This proves the inconsistency was due to the tensioning of the wire. Added fins could only have possible increased the load due to added water resistance, decreasing tail beat frequency for the same voltage input. But the results of this experiment are not completely inconclusive on the effects of stabilizing fins. We can still conclude something based on this comparison. A longer tail beat amplitude is more efficient because it maintains the ideal angle for a longer period. Thus less work should need to be exerted for the same speed. Stabilizing fins should have a similar effect on efficiency. In graph 7.5b we can see the speed compared to voltage input is similar. Concluding that the increased efficiency due to increased tail beat amplitude of approximately 11% is about the same as of the added stabilizing fins. As there is not reference footage we can't quantify the amount it increases efficiency. It could possibly still be very low.

7.4. Experiment #10: Influence propulsor surface area

We increase the caudal fin surface area and compare these results with the smaller tail. Increased surface area should increase speed with the same frequency. Depending on frequency and compliant tail stiffness an optimum could be found where the caudal fin reaches the most efficient angle of attack due to the compliant tail deforming creating a S-shape tail. In previous experiments with a smaller caudal fin the compliant tail only started to minimally deform at its highest frequencies. Due to the new backbone material the frequency can also be increased further increasing the chance of high performance.

7.4.1. Hypotheses

Due to the chord ratio of the tail being the same, the produced propulsive thrust due to the shape is linear with increased surface area. However due to the higher resistance of the surrounding water the large till is suspected to bend further creating a closer to ideal angle of attack. Thus the hypothesis is that the large tail will perform better than calculations only taking into account the increase of surface area.

7.4.2. Method

We estimate the speed of the fish of the large tail experiment without change of angle based on the experimental data of the small tail experiments and than solving the input and output force equation for the larger tail. Hydrodynamic drag is commonly expressed as:

$$F_{\mathrm{D}} = (1/2)\rho S v^2 C_{\mathrm{D}}$$

Where ρ is density of the fluid, v, speed, S, reference area and C_{D} the respective drag coefficient. Only the speed changes. The resistance of the surrounding water increases quadratically with a linear increase of the speed. The thrust force (F_{t}) and drag forces are in equilibrium when swimming at a constant speed. There is a power law relation between:

$$F_{\mathrm{t}} = F_{\mathrm{D}}$$

Where with the same body and in the same fluid

$$F_{\mathrm{D}} = v^2 x$$

Where F_{t} increases linearly with surface area of the caudal fin. X is a constant value which replaces all non changing values. Filling in the speed from the experiment with the small tail, and surface area as F_{t} will give us the value for x. By using this x value and changing the F_{t} surface area for the large tail we can estimate the speed of the large tail not taking into account change of angle of attack. These results are compared to the measured data retrieved by the same method as described in experiment 8.

Table 7.2: comparison of caudal fin surface area

	tail small	tail large
Caudal fin surface area	2430.93mm^2	4064.86mm^2

7.4.3. Results

A new top speed of 0.85 m/s was reached. Analyses of the footage shows the caudal fin deforms in a nice S-shape not over bending at the top of the heave amplitude. The footage is not of good enough quality to determine exact angle of attack. Exact values for both speed and frequency be found in appendix D. Exact values for the predicted large tail performance as depicted in graph 7.7b can be found in appendix E.

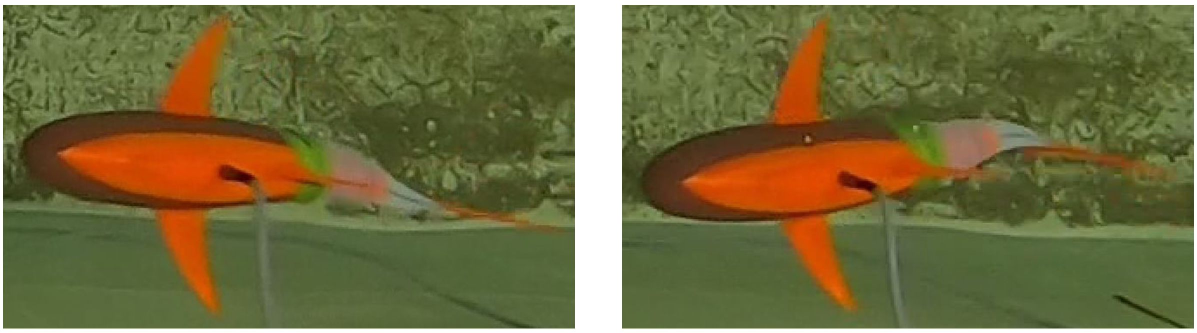

(a) (b)

Figure 7.6: Showing the S-shape bending of the tail at 4.7 Hz.

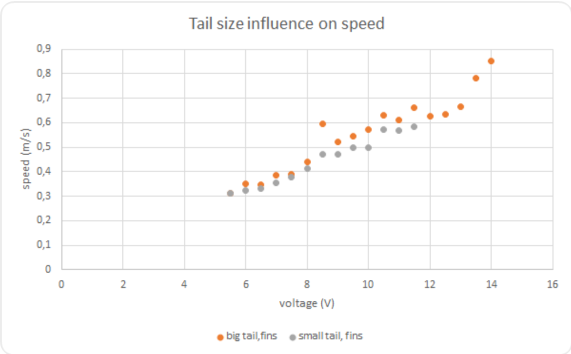

(a)

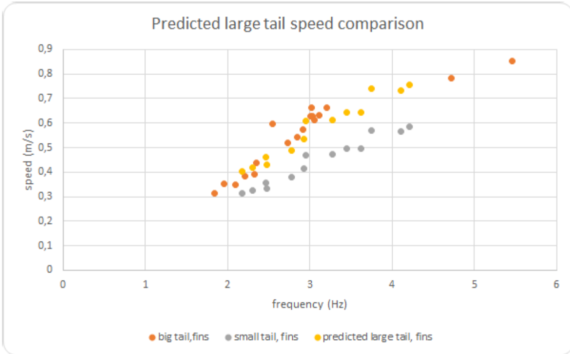

(b)

Figure 7.7: (a) Graph displaying the speed, voltage relation. Showcasing the big tail has a higher speed output for the same voltage input. (b) Comparison of both small tail, large tail and predicted large which is calculated based on the increased surface area from the small tail data.

7.4.4. Conclusion

The increase of caudal fin surface area has a clear positive impact on speed. The speed, voltage graphs show a clear higher performance for the same voltage input indicating higher efficiency is achieved. Comparing the performance with the predicted speed values for the large tail it shows that it starts to exceed the predictions from around 2.5 Hz. In the footage we can see the deformation slowly starts to occur at this speed. Concluding that the increase of performance can be related to both increase in caudal fin surface area and deformation of the compliant tail.

7.4.5. Discussion

In this comparison we are not able to properly compare the angle of attack due to the quality of the footage. Increased footage quality and analyzing set-up for instance with a laminar flow tank would allow for a better analyses enabling taking into account the exact angle of attack. This would enable us to get to more precise conclusion than an adaptation makes performance better or worse.

8
Conclusion & recommendations

8.1. Conclusion

In this thesis we investigated if a compliant active body can potentially mimic the efficient oscillating movement of a real fish, we identified the main parameters with a strong influence on speed and efficiency and used these parameters to design the fastest swimming soft robotic fish, swimming up to 0.85 m/s. This is the first soft robotic fish which uses a simple dc-motor to drive the system instead of a servo motors enabling it to reach high tail beat frequencies and have lower internal loses.

8.2. Recommendations

The parameters to optimize are identified but are still far from completely optimized in our final prototype, leaving room for further improvement. Some identified parameters with high influence on speed were not implemented in the final design at all due to their complexity. Especially caudal fin design has shown a high potential for further research. There is little known on the subject, but it is clear that a more flexible caudal fin with fin rays would be more efficient. Due to the focus on motion, shape and skin structure have barely been taken into account. Of course the shape and skin friction has a high influence on the performance of a robotic fish. Optimizing these parameters shows another opportunity for increased performance.

In this thesis the numerical model is used to analyse if a compliant/active body can create a similar movement as that of a real fish and is used to investigate the influence of different factors of stability. The numerical model has however greater potential in analyzing, predicting and optimizing the behaviour of the (robotic) fish. If a laminar flow tank would be available this would allow for stable top view footage to be generated of the robotic fish. This footage could then be used to create a numerical copy of the robotic fish. Enabling for fast optimization by changing parameters such as frequency and compliant tail stiffness to generate the right angle for efficient thrust.

During testing not all variables could be properly controlled, making it difficult to draw conclusions based on the experimental data, most notable wire tightening. A system allowing for precise wire tightening would be advised in future research. Other prototype related recommendation would be if the prototype is tested for an extended time to change the material of the body from PLA to a more durable material such as ABS or Nylon.

9 Glossary

Term	Definition
Chord-ratio	Ratio between the height of the caudal fin (or other wing) to the length of the chord.
AUV	Autonomous underwater vehicle
Caudal fin	Fin add the end of the tail, responsible for the propulsive force
Anal fin	Stabilizing fin on the bottom of a fish
Dorsal fin	Stabilizing fin on the top of a fish
Pectoral fins	Stabilizing fins on the side of a fish. In some fish they also aid in thrust production and steering.
Multilink	A segmented/linked system of multiple systems, in this case often servo's.
Thunniform swimming	A highly efficient swimming motion created by tuna and fast swimming fish.
Carangiform swimming	A slightly less efficient swimming motion actuating a larger part of the fish.
Von karman vortex	A repeating pattern of swirling vortices, caused by a process known as vortex shedding.
Reverse von karman vortex	Similar as a von karman vortex only the vortices turn inwards creating a high pressure area behind the object.
Strouhal number	A dimensionless number describing the relation between heave amplitude, tail beat frequency and speed in oscillating flow mechanisms.
Cavitation	The creation of small vapor-filled cavities created in low pressure zones in liquids. Collapsing of these cavities creates shock waves which can damage an object.
Pelagic	Pelagic fish live in the pelagic zone of ocean, being neither close to the bottom nor near the shore. Pelagic fish in general travel very large distances.

10

appendices

10.0.1. Appendix A: Arduino code for servo steering with joystick & potmeter speed control

```
#include <Servo.h>
//middle of the servo seems to be around 75
Servo myservo;  // create servo object to control a servo

int pos = 0;
int joyX;  // analog pin used to connect the potentiometer
int servo1 = 9;    // variable to read the value from the analog pin
int potS;      //value of the potmeter to determine the Speed of the tail going left to recht


void setup() {
  myservo.attach(servo1);  // attaches the servo on pin 9 to the servo object
}

void loop() {

  potS = analogRead(0);           // reads the value of the potentiometer from A1 (value between 0 and
1023)
    potS = map(potS, 0, 1023, 20, 2);     // converts reading from potentiometer to an output value in
degrees of rotation that the servo can understand
//    Serial.print("snelheid ");
 // Serial.println(potS);

  joyX = analogRead(3);           // reads the value of the potentiometer (value between 0 and 1023)
  joyX = map(joyX, 0, 1023, -2, 20);     // scale it to use it with the servo (value between 0 and 180)

  for (pos = 40+joyX; pos <= 120+joyX; pos += 1) { // goes from 0 degrees to 180 degrees
    // in steps of 1 degree
    myservo.write(pos);            // tell servo to go to position in variable 'pos'
    delay(potS);                   // waits 15ms for the servo to reach the position
  }
  for (pos = 120+joyX; pos >= 40+joyX; pos -= 1) { // goes from 180 degrees to 0 degrees
    myservo.write(pos);            // tell servo to go to position in variable 'pos'
    delay(potS);                   // waits 15ms for the servo to reach the position
  }
}
```

10.0.2. Appendix B: Receiver code 2 servo’s and 1 DC-motor speed control

```
[code]

// works without jitter only with external powersupply
#include <Servo.h>    //the library which helps us to control the servo motor
#include <SPI.h>     //the communication interface with the modem
#include "RF24.h"     //the library which helps us to control the radio modem

Servo myServo;       //define the servo name
Servo myServoTwo;    //define the servo name
int motorPin = 9;        //define motorname

RF24 radio(5, 10);    /*This object represents a modem connected to the Arduino.
                Arguments 5 and 10 are a digital pin numbers to which signals
                CE and CSN are connected.*/

const uint64_t pipe = 0xE8E8F0F0E1LL; //the address of the modem,that will receive data from the
Arduino.

int msg[3];



void setup() {
  myServo.attach(3);             //3 is a digital pin to which servo signal connected
  myServoTwo.attach(6);          //6 is a digital pin to which servo signal connected
  pinMode(motorPin, OUTPUT);

  radio.begin();                //it activates the modem.
  radio.openReadingPipe(1, pipe);   //determines the address of our modem which receive data.
  radio.startListening();         //enable receiving data via modem
}

void loop(){
  if(radio.available()){          //checks whether any data have arrived at the address of the modem
     radio.read(&msg, sizeof(msg));
     analogWrite(motorPin, msg[2]);
     myServo.write(msg[1]);
    myServoTwo.write(msg[0]);
    }
  }
//}
[/code]
```

10.0.3. Appendix C: Transmitter code 2 servo's and 1 DC-motor speed control

```
[code]

#include <SPI.h>                  //the communication interface with the modem
#include "RF24.h"                  //the library which helps us to control the radio modem

int msg_Pin = A0;                 // connects to analoge pin A0
int msgTwo_Pin = A1;                // connects to analoge pin A1
int msgThree_Pin = A2;              // connects to analoge pin A2, dc-motor
int sensorValue = 0;              // sets initial value

int msg[3];                     // creates an array of 2, holding data of both potmeters


RF24 radio(5,10);                 //5 and 10 are a digital pin numbers to which signals CE and CSN are
connected.

const uint64_t pipe = 0xE8E8F0F0E1LL; //the address of the modem, that will receive data from
Arduino.


void setup(void){
  radio.begin();                  //it activates the modem.
  radio.openWritingPipe(pipe);       //sets the address of the receiver to which the program will send
data.
}

void loop(void){
  // writes data in the array &maps input over 180 degrees
  msg[0] =  map (analogRead(msg_Pin), 0, 1023, 0, 180);
  msg[1] =  map (analogRead(msgTwo_Pin), 0, 1023, 0, 180);

  sensorValue = analogRead(msgThree_Pin)/4;
 msg[2] =  map (analogRead(sensorValue), 0, 1023, 0, 255);


  radio.write(&msg, sizeof(msg));
}
[/code]
```

10.0.4. Appendix D: Experimental data and calculations

Small tail

video t tel	voltage	fu l seconds	frames	total seconds	head L begin	head L end	projec ed L	str distance (px)	prj distance (M)	speed (m s)	speed (BL/s)	distance with a	degrees screen	hz	strohaul nr.	tail sweep L px	reference L px	tail sweep m
11 0V_tes 2.MP	11	3	96	3 96969697	19	1	182 814519	2096.1	2 8 7 13857	0.717287 08	1 7 73931	1928 28247	-1	2.968876872	0. 5665112	76	175	0.1077 62857
10 5V_tes 3	10.5		10	.101010101	189	151	180. 68356	2065.2	2 838201582	0.692317622	1.686563917	1934 418865	7	2.78 375	0. 376372262	75	171	0.1088157895
10 0V_test1.MP	10	3	96	3 96969697	198	13	183 70693 (	2161.6	2 919253552	0.73538 82	1.791 79853	1938	0	2.793103 8	0 3935560056	71	170	0.1036182353
9.5V_ est3.MP	9.5	3	91	3.919191919	133	200	185 06	217 .38	2 91507 52	0.7 379 7691	1.811968062	1938		2.716 63 15	0. 31 775556	80	168	0.1181 28571
9.0V_ est1.MP	9	6	11	6.111111111	1 9	192	182 37 0 8	2068.63	2 81 1 5 71	0. 60 965311	1.121821559	1938		2.372727273	0 5202569606	70	172	0.1009709302
8.5V_ est1.MP	8.5	6	8	6.8 8 8 8 8 8	1 5	20	190 85	2175.16	2 82765101	0. 1288709	1.00583959	1962 893942	12	2.338283186	0 568 303655	66	163	0.100 576687
8.0V_ est3_beter.MP	8	6	15	6.151515152	165	193	186 7509511	2012. 2	2.67351 63	0. 3 610752	1.058760878	1923 587879	3.5	2.113300 93	0 53932707 2	76	170	0.11091529 1
7.5V_ est1	7.5	7	98	7 98989899	1 7	185	176. 1678	206 .31	2.90268896	0.36329 825	0.885027225	1938 575897	-6	2.127686 73	0 6321632809	67	15	0.107939610
7.0V_ est2.MP	7	7	20	7.202020202	161	193	185 85 225	2025.91	2 70 2206	0.375508816	0.91 781888	1922 294956	2.8	2.013323983	0 5573506671	75	179	0.10395251
6.5V_ est1	6.5	9	29	9.292929293	163	183	178 507900	198 .89	2 758706197	0.296890990	0.723188900	1928 748871	1.6	1.85625	0 5856093562	57	151	0.0938536 238
6.0V_ est2.MP	6	9	2	9 02020202	17	192	187 98197	1992.85	2.83017817	0.291587501	0.7103 0085	1937 938838	7.8	1.718365082	0 5 15136006	70	189	0.09188888889
5.5V_ est1.MP	5.5	10	23	10 23232323	16	166	165 5 69	1932.32	2 895907999	0 283015688	0.689 58179	1925 937821	.5	1.697889182	0 59726 2122	63	157	0.0995593096

La ge tail fins

video t tel	voltage	fu l seconds	frames	total seconds	head L begin	head L end	projec ed L	str distance (px)	prj distance (M)	speed (m s)	speed (BL/s)	distance with a	degrees screen	begin fu l s	begin frames	end fu l s	end frames	full cycles	hz
sh_1 .0V_metig.MP	1	1	68	1.686868687	185	162	188 589558	10 7.39	1. 389 685	0.853028253	2.078073165	1884 523884	.8	0	67	3	2	1	5. 58892913
sh_13.5V_ est3.MP	13.5	3	3	3. 3 3 3 3	17	181	179 429571	19 2.17	2 685 68522	0.7819 663	1.90 905513	1928 947872	1.8	0	61	3	37	13	.71 28571
sh_13.0V_ est1.MP	13	3	95	3 95959596	175	189	185 872364	1969.65	2 629063055	0.663972557	1.617512137	1927 334888	5	0	56	3	68	10	3.203883 95
sh_12.5V_ est2_goed.MP	12.5		13	.131313131	181	18	183 328796	1935.01	2 618681069	0.633856835	1.5 1 6839	1926 284539	.6	0	76	3	97	10	3.1132075 7
sh_12.0V_ est1.MP	12		35	.35353535	176	175	175 775982	1935.0751	2 731287932	0 627372 02	1.528350026	1932 848633	6.	0	76		7	10	3.027522936
sh_11.5V_ est2.MP	11.5		3	.3 3 3 3 3	162	175	172 959957	1997.285 23	2 879033 95	0.66305 55	1.615275538	1954 621725	10.8	0	77	3	91	9.5	3.02 115756
sh_11V_test2_goed MP	11		35	.35353535	17	185	182 537347	1955.991986	2 658533271	0.61088077	1. 8763861	1922 634984	3	0	69		30	11	3.050 20168
sh_10.5V_ est2.MP	10.5		23	.232323232	17	185	182 536996	1958.077392	2 681372968	0.62862082	1.531878535	1924 888444		0	71		20	10.5	3.0130 3 78
sh_10.0V_ est2_goed.MP	10		52	.525252525	178	190	187 323606	1955.9088 8	2 590 958 2	0 572 53278	1.39 560837	1928 28247	1	0	77		37	10.5	2.9199 382
sh_9.5V_test1.MP	9.5		86	.868686869	178	183	181 660111	19 0.308515	2.6 67 6 7	0.5 38283 9	1.32 33518	1925 4198	.3	1	1		69	10.5	2.8 79 5305
sh_9.0V_tes 3.MP	9	5	11	5.111111111	179	181	180 5515306	1938.51811	2 68101395	0 520633165	1.288321189	1938 575897	6	0	95		98	11	2.729323308
sh_8.5V_tes 2.MP	8.5		5	.5 5 5 5 5	178	178	178	19 3.8330 2	2 709 93189	0.596088501	1. 52138911	1943 933842	9	0	78		51	9.5	2.5 6760 88
sh_8.0V_tes 3.MP	8	6	11	6.111111111	180	177	179 326533	19 2.6189 9	2 687629 09	0. 397939033	1.071387818	1933 681987	6.8	1	8	5	97	11.5	2.3 7 2288
sh_7.5V_test1.MP	7.5	6	93	6.939393939	178	178	178	19 2.870733	2 706012522	0.390237612	0.950862898	1942 879733	8.8	1	23	6	80	13	2.331521739
sh_7.0V_tes 3.MP	7	7	35	7.35353535	175	169	173.6 502	1979.051182	2 827622689	0.38 525612	0.9367 7820	1968 833189	11.6	1	13	7	22	13.5	2.216 1791
sh_6.5V_tes 2_oke sh.MP	6.5	7	93	7.939393939	179	17	177 87 312	1975. 73501	2 755 00535	0.3 705 285	0.8 5 633873	1947 28949	9.6	1	1	7	81	1	2.096822885
sh_6.0V_tes 2.MP	6	7	88	7.888888889	17	170	173 098350	1939.759873	2 780238913	0.352 2 397	0.8585 583	1927 334888	5	1	20	7	8	13	1.955927052
sh_5.5V_tes 3.MP	5.5	8	75	8.757575758	178	171	176. 262769	19 1.8 186	2 730721151	0.311812 9	0.7598103 3	1928 28247	1	1	5	8	53	13	1.8359 86 5

Small tails fins

video t tel	voltage	fu l seconds	frames	total seconds	head L begin	head L end	projec ed L	str distance (px)	prj distance (M)	speed (m s)	speed (BL/s)	distance with a	degrees screen	begin fu l s	begin frames	end fu l s	end frames	full cycles	hz
se_11.5V_test2.MP	11.5		58	.585858586	175	189	185 863498	2009.699308	2 6826 8561	0.58 982635	1. 2508 255	1966 816667	12.5	0	65		5	16	.212765957
se_11V_tes 2.MP	11		75	.757575758	173	183	189 756348	1965.92 919	2 698361628	0.567171552	1.361693957	1935 269084	7.2	1			69	15	.1022099 5
se_10.5V_test2.MP	10.5		58	.585858586	186	183	183 329687	1956. 3383	2 621760505	0.571705 8	1.392739128	1949 819995	10	0	79		53	1	3.7 59 59 6
se_10.0V_test1.MP	10	5	27	5.272727273	186	180	18 656219	19 9. 03365	2.6191 677	0. 9673 732	1.210101906	1931 665413	6.3	0	82	5	11	15.5	3.01910377
se_9.5V_test3.MP	9.5	5	3	5.3 3 3 3 3	185	179	183 6557	1965.9075 3	2 655603568	0. 9698 1	1.210710162	1947 842461	9.7	0	69	5	25	15	3. 5 75638
se_9.0V_test1.MP	9	5	65	5.656565657	182	179	181 327007	1953. 3182	2 672791327	0. 725113231	1.1510959 9	1944 473519	9.1	0	91	5	9	15	3.2781 5895
se_8.5V_test1_best.MP	8.5	5	66	5.666666667	179	180	179 7757	1927. 195 8	2 6599 0505	0. 69 01265	1.1 351 98	1924 456595	3.9	0	86	5	60	1	2.955223881
se_8.0V_test2.MP	8	6	55	6.555555556	180	173	178. 27 15	1952.731726	2 715237115	0. 1 1887	1.039010 81	1931 298231	6.2	1	6	6	52	16	2.927911275
se_7.5V_test2.MP	7.5	7	7	7.070707071	183	177	181 65 701	1955.98888	2.671 68	0.377918881	0.920 09 69	1937 939838	7.8	1	5	6	97	16.5	2.782793987
se_7.0V_test1_best.MP	7	7	1	7. 1 1 1 1	183	178	181 880283	1938.06227	2 6 367990	0.356572630	0.888511977	1923 189	3.3	1	2	8	1	17	2. 6 1288 3
se_6.5V_test2.MP	6.5	8	18	8.181818182	182	170	179 3058162	1965 174693	2 719152	0.3323 08 8	0.8098188 1	1927 93461	5.2	1	25	8	13	17	2. 71365639
se_6.0V_test3.MP	6	8	8	8. 8 8 8 85	183	18	178 7319 1	1966.166326	2 757021635	0.32 93 716	0.7915776	1925 4198	.3	1	31	8	25	16	2.305676856
se_5.5V_test1_met g.MP	5.5	8	80	8.808080808	181	189	178 3019	1975.5 1 65	2 7 8666907	0.312086930	0.7652790	1937 939838	7.8	1	6	9	29	17	2.171612903

10.0.5. Appendix E: Predicted large tail performance data

side+S tail					variabe value X for		predicted L tail		actual L tail			
video titel	voltage	frequency (Hz)	speed (m/s)	speed (BL/s)	m/s	BL/s	speed(m/s)	speed (BL/s)	speed (m/s)	speed (BL/s)	frequency (Hz)	voltage
ss_11.5V_test2.M	11,5	4,212,765,957	58,498,284	1,425,084,255	7,103,726	1,196,992	75,644,907	1,842,795,366	853,028,254	2,078,073,165	5,456,693	14
ss_11V_test2.MF	11	4,102,209,945	56,717,155	1,381,693,957	7,556,898	1,273,353	733,417,063	1,786,686,796	781,944,664	1,904,905,513	4,714,286	13,5
ss_10.5V_test2.M	10,5	3,745,945,946	57,170,548	1,392,739,128	7,437,513	1,253,236	73,927,995	1,800,969,452	663,972,557	1,617,512,137	3,203,883	13
ss_10.0V_test1.M	10	3,619,103,774	49,673,473	1,210,101,908	9,851,977	1,660,078	642,334,275	1,564,798,839	633,856,836	1,544,146,839	3,113,208	12,5
ss_9.5V_test3.M	9,5	3,445,475,638	49,698,441	1,210,710,162	9,842,081	1,658,411	642,657,143	1,565,585,381	627,372,402	1,528,350,026	3,027,523	12
ss_9.0V_test1.M	9	3,278,145,695	47,251,132	1,151,090,949	10,887,997	183,465	611,010,665	1,488,490,985	663,054,456	1,615,275,538	3,024,116	11,5
ss_8.5V_test1_b	8,5	2,955,223,881	46,940,127	1,143,514,496	11,032,754	1,859,042	606,989,007	1,478,693,773	610,660,775	1,487,638,614	305,042	11
ss_8.0V_test2.M	8	2,927,911,275	41,418,871	1,009,010,481	14,170,199	2,387,707	535,592,922	1,304,764,846	62,882,082	1,531,878,535	3,013,043	10,5
ss_7.5V_test2.M	7,5	2,782,793,867	37,781,888	920,409,467	17,029,627	2,869,527	488,562,611	1,190,193,698	572,453,278	1,394,560,837	2,919,944	10
ss_7.0V_test1_b	7	2,464,128,843	35,657,263	868,651,198	19,119,496	3,221,674	461,088,801	1,123,264,394	54,362,635	1,324,335,184	2,847,945	9,5
ss_6.5V_test2.M	6,5	2,471,365,639	33,234,085	809,619,842	22,009,238	3,708,601	429,754,363	1,046,930,164	520,633,165	1,268,321,189	2,729,323	9
ss_6.0V_test3.M	6	2,305,676,856	32,493,472	791,577,666	23,023,971	3,879,586	420,177,395	1,023,599,587	596,088,502	1,452,138,911	254,878	8,5
ss_5.5V_test1_m	5,5	2,171,612,903	31,208,693	76,027,901	24,958,661	4,205,585	403,563,753	98,312,688	439,793,903	1,071,387,618	2,347,423	8
									390,237,612	950,662,896	2,331,522	7,5
									384,525,613	936,747,821	2,216,418	7
									347,054,266	845,463,387	2,096,823	6,5
									352,424,397	858,545,634	1,955,927	6
									31,181,245	759,610,343	1,835,949	5,5

10.0.6. Appendix F: Project brief

Start 1/2/17

2847

DESIGN FOR our future

TUDelft

IDE Master Graduation

Project team, Procedural checks and personal Project brief

This document contains the agreements made between student and supervisory team about the student's IDE Master Graduation Project. This document can also include the involvement of an external organisation, however, it does not cover any legal employment relationship that the student and the client (might) agree upon. Next to that, this document facilitates the required procedural checks. In this document:

- The student defines the team, what he/she is going to do/deliver and how that will come about.
- SSC E&SA (Shared Service Center, Education & Student Affairs) reports on the student's registration and study progress.
- IDE's Board of Examiners confirms if the student is allowed to start the Graduation Project.

USE ADOBE ACROBAT READER TO OPEN, EDIT AND SAVE THIS DOCUMENT

Download again and reopen in case you tried other software, such as Preview (Mac) or a webbrowser.

STUDENT DATA & MASTER PROGRAMME

Save this form according the format "IDE Master Graduation Project Brief_familyname_firstneme_studentnumber_dd-mm-yyyy". Complete all blue parts of the form and include the approved Project Brief in your Graduation Report as Appendix 1 !

family name
initials
student number
street & no.
zipcode & city
country
phone
email

[redacted]

Your master programme (only select the options that apply to you):

IDE master(s): (★) IPD ( ) Dfl ( ) SPD

2nd non-IDE master:

individual programme: - - (give date of approval)

honours programme: ( ) Honours Programme Master

specialisation / annotation: ( ) Medisign
( ) Tech. in Sustainable Design
(★) Entrepeneurship

SUPERVISORY TEAM **

Fill in the required data for the supervisory team members. Please check the instructions on the right !

** chair: Zoltan Rusak — dept. / section: IDE

** mentor: Jun Wu — dept. / section: IDE

2nd mentor:

organisation:

city: country:

comments (optional)

Chair should request the IDE Board of Examiners for approval of a non-IDE mentor, including a motivation letter and c.v..

Second mentor only applies in case the assignment is hosted by an external organisation.

Ensure a heterogeneous team. In case you wish to include two team members from the same section, please explain why.

10.0.7. Appendix F: Project brief

TUDelft

Procedural Checks - IDE Master Graduation

APPROVAL PROJECT BRIEF
To be filled in by the chair of the supervisory team.

chair Zoltan Rusak date 14-09-2018 signature

CHECK STUDY PROGRESS
To be filled in by the SSC E&SA (Shared Service Center, Education & Student Affairs), after approval of the project brief by the Chair.
The study progress will be checked for a 2nd time just before the green light meeting.

Master electives no. of EC accumulated in total: 24 EC

Of which, taking the conditional requirements into account, can be part of the exam programme 24 EC

List of electives obtained before the third semester without approval of the BoE

YES all 1st year master courses passed

NO missing 1st year master courses are:

name date 8-10-18 signature

FORMAL APPROVAL GRADUATION PROJECT
To be filled in by the Board of Examiners of IDE TU Delft. Please check the supervisory team and study the parts of the brief marked **.
Next, please assess, (dis)approve and sign this Project Brief, by using the criteria below.

- Does the project fit within the (MSc)-programme of the student (taking into account, if described, the activities done next to the obligatory MSc specific courses)?
- Is the level of the project challenging enough for a MSc IDE graduating student?
- Is the project expected to be doable within 100 working days/20 weeks ?
- Does the composition of the supervisory team comply with the regulations and fit the assignment ?

Content: APPROVED NOT APPROVED

Procedure: APPROVED NOT APPROVED

comments

name A Kuiwae date 16-10-2018 signature

Initials & Name S.C. van den Berg Student number 4172272

Title of Project Design of a soft robotic oscillating marine propulsion system

10.0.8. Appendix F: Project brief

Personal Project Brief - IDE Master Graduation

TUDelft

Design of a soft robotic oscillating marine propulsion system — project title

Please state the title of your graduation project (above) and the start date and end date (below). Keep the title compact and simple. Do not use abbreviations. The remainder of this document allows you to define and clarify your graduation project.

start date 03 - 09 - 2018 — 03 - 03 - 2019 end date

INTRODUCTION **

Please describe, the context of your project, and address the main stakeholders (interests) within this context in a concise yet complete manner. Who are involved, what do they value and how do they currently operate within the given context? What are the main opportunities and limitations you are currently aware of (cultural- and social norms, resources (time, money,...), technology, ...).

This graduation project builds further on the research done in the research elective (9ec) course with soft robotics research group. Together with Tommie Perenboom we also investigated the market potential of oscillating propulsion as part of the elective Build Your Start-up (15ec) and identified beachhead markets.
I am confident there is a need, but the technology is still immature. I believe I can contribute to the future implementation of the technology by optimizing the technology and showcasing its potential.

Opportunities
The soft robotic propulsion system has three major benefits compared to traditional propeller propulsion: higher efficiency, less noise and better safety.

Efficient propulsion
According to research, oscillating propulsion technology can be significantly more efficient (86%) than rotor propulsion (40%)^1.
1. Triantafyllou, M. S., & Triantafyllou, G. S. (1995). An efficient swimming machine. Scientific american, 272(3), 64-70.

Silent propulsion
The relatively slow moving tail produces much less noise and vibrations in the water.

Safe propulsion
This propulsion uses a soft tail instead of fast moving sharp rotor blades which could harm its environment and easily entangle itself. Because there are no external rotating parts, it can be made watertight much better, with less losses at high depth.

Limitations
Although oscillation has been proven to be very efficient in lab tests with foils and analyses of fish swimming, nobody has been able to produce an oscillating propulsion system (OPS) which produces significant speed and efficiency in a simple manner. This will be the hardest challenge of this assignment. If I am able to design a simpler efficient OPS it can be a more efficient alternative for marine propulsion in general.

Other limitations
Oscillating propulsion creates some swaying motion in the craft it is pushing. This instability could be an issue for many applications. This problem could be negotiated by creating a 4 tail sweeping propulsion in different horizontal shifts in frequency or the of a sail. However the added complexity may reduce its efficiency and increase its price not enabling it to compete with rotator blade propulsion in most common applications.

space available for images / figures on next page

10.0.9. Appendix F: Project brief

Personal Project Brief - IDE Master Graduation

introduction (continued): space for images

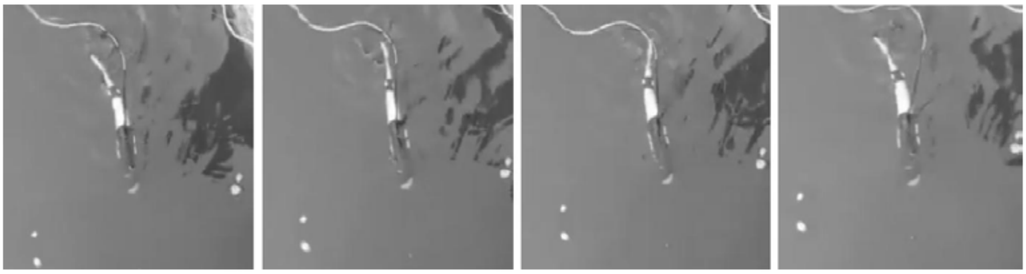

image / figure 1: Prototype 2, experimental result of research elective. source: https://youtu.be/a7Nuj0JUkGo

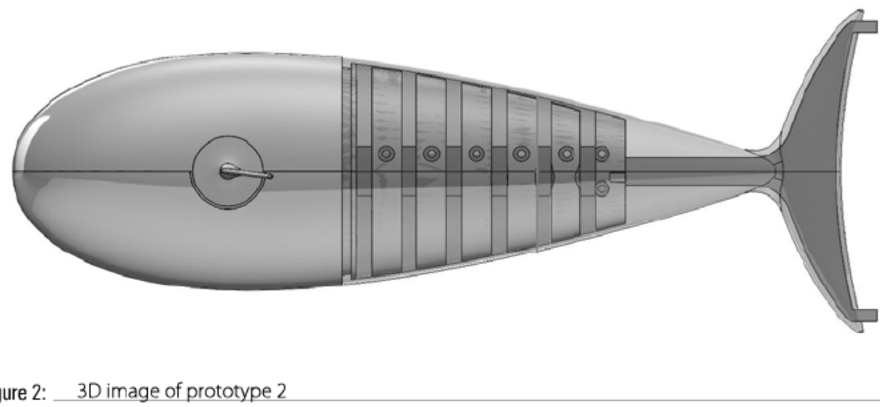

image / figure 2: 3D image of prototype 2

10.0.10. Appendix F: Project brief

TUDelft

Personal Project Brief - IDE Master Graduation

PROBLEM DEFINITION **

Limit and define the scope and solution space of your project to one that is manageable within one Master Graduation Project of 30 EC (= 20 full time weeks or 100 working days) and clearly indicate what issue(s) should be addressed in this project.

During the elective Build Your Start-up we investigated different markets from a technology push perspective of oscillating propulsion using the 3 main benefits of oscillating propulsion as described in the introduction. We have defined markets, two of which we have identified as promising beachhead markets; robotic recreational fishing lure and shore inspection for the marines.

Problem recreational fishing:
For recreational fishing the consumer appeal is a lure which exactly mimics a fish to the exact spot you want. The design challenge is creating a cheap remote controlled lure which accurately mimics the swimming motion of a fish .

Problem marines:
For the marines the largest benefit is stealth. The similar look and vibration profile it produces compared to fish, making it almost undetectable.

For both markets it has to swim first. The main design challenge is there for higher speed and efficient swimming. The goal speed is 2m/s, the cruising speed of tuna. I am going to achieve this speed by high frequency tail beat and the mimicking of motion of Thunniform swimming (most efficient in nature) and theoretical and experimental data of foils. Efficiency of motion defined as strouhal number (relation between speed, tail beat frequency and tailtip sweep length). With a target strouhal number of between 0.2 and 0.4. This unit is often referred to as an indication of efficient swimming. Highest efficiency will most likely occur at lower than topspeed. For reference the in 2018 launched soft robotic fish SoFi from MIT had a total range of 521 meter before the battery ran out and a speed of 21.7 cm/s.

ASSIGNMENT **

State in 2 or 3 sentences what you are going to research, design, create and / or generate, that will solve (part of) the issue(s) pointed out in "problem definition". Then illustrate this assignment by indicating what kind of solution you expect and / or aim to deliver, for instance: a product, a product-service combination, a strategy illustrated through product or product-service combination ideas, ... In case of a Specialisation and/or Annotation, make sure the assignment reflects this/these.

Design a controllable single motor driven (simple) soft robotic oscillating marine propulsion system for high speed and efficiency. Building a watercraft prototype showcasing the potential of oscillating propulsion and its potential to move efficiently and at high speeds.

I already executed a significant amount of literature research as part of my research elective. I will build further on this knowledge of fish kinematics by analyzing steady tuna reference footage obtained from the Monterey bay aquarium (revised request currently in review at the aquarium). I will reproduce the concluded target movement first with a numerical model consisting of an active and compliant component for faster optimization. IF the movement of the numerical model is as desired I will reproduce this movement with a prototype.

Current robotic fish prototypes generally consist of a linked servos to mimic the motion of the tail. This limits the tail sweep frequency. I am going to replace the linked servos by a single dc-motor with a compliant and active body part. With the right stiffness distribution in the compliant tail the desired sweeping motion can be achieved. the dc-motor allows for higher frequency movement, is cheaper and decreases power consumption.

The created prototype will serve as a showcase of the potential of oscillating propulsion and soft robotics. I intend to use the prototype to obtain interest from different stakeholders, and as bases on which new products can be designed for the specified beachhead markets marine defense and recreational fishing.

10.0.11. Appendix F: Project brief

TU Delft

Personal Project Brief - IDE Master Graduation

PLANNING AND APPROACH **

Include a Gantt Chart (replace the example below - more examples can be found in Manual 2) that shows the different phases of your project, deliverables you have in mind, meetings, and how you plan to spend your time. Please note that all activities should fit within the given net time of 30 EC = 20 full time weeks or 100 working days, and your planning should include a kick-off meeting, mid-term meeting, green light meeting and graduation ceremony. Illustrate your Gantt Chart by, for instance, explaining your approach, and please indicate periods of part-time activities and/or periods of not spending time on your graduation project, if any, for instance because of holidays or parallel activities.

start date 3 - 9 - 2018 3 - 3 - 2019 end date

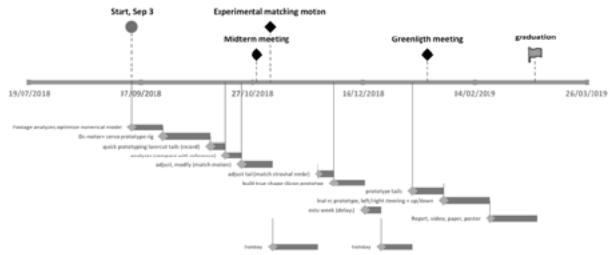

Tasks

Start	End	Duration (weeks)	Label
03/09/2018	16/09/2018	2	Footage analyses, optimize numerical model
17/09/2018	07/10/2018	3	Dc-motor+ servo prototype rig
08/10/2018	14/10/2018	1	quick prototyping lasecut tails (record)
15/10/2018	21/10/2018	1	analyses (compare with reference)
22/10/2018	04/11/2018	2	adjust, modify (match notion)
26/11/2018	02/12/2018	1	adjust tail (match strouhal nmbr)
03/12/2018	16/12/2018	2	build true shape silicon prototype
07/01/2019	20/01/2019	2	prototype tails
21/01/2019	10/02/2019	3	final rc prototype, left/right steering + up/down
17/12/2018	23/12/2018	1	extra week (delays)
11/02/2019	03/03/2019	3	Report, video, paper, poster
		21	
24/12/2018	06/01/2019	2	holiday
05/11/2018	25/11/2018	3	holiday

because a large part of the literature research has already been executed as part of the research elective it has not been included in the planning.

10.0.12. Appendix F: Project brief

Personal Project Brief - IDE Master Graduation

TUDelft

MOTIVATION AND PERSONAL AMBITIONS

Explain why you set up this project, what competences you want to prove and learn. For example: acquired competences from your MSc programme, the elective semester, extra-curricular activities (etc.) and point out the competences you have yet developed. Optionally, describe which personal learning ambitions you explicitly want to address in this project, on top of the learning objectives of the Graduation Project, such as: in depth knowledge a on specific subject, broadening your competences or experimenting with a specific tool and/or methodology, ... Stick to no more than five ambitions.

I want to gain further experience in the field of (soft) robotics. I was drawn to robotics due to the complexity and multidisciplinary nature of the field. I chose this subject because I believe in its market potential and abilities to teach me skills such as mechatronics, biomechanics and numerical modeling. Which I believe are valuable skills in a high tech multidisciplinary fields in which I would like to work.

This project is in line with my development throughout my education. I am specializing in high-tech interdisciplinary industries. I believe robotics is such an area. I have previously been part of the University Racing Team Eindhoven in Delft known as the DUT and spend 1 and half year full-time as interior and exterior designer at Solar Team Eindhoven. I am still involved with Solar Team as part of the management of the foundation Solar Team Eindhoven and in an advisory role for new members.

I have entrepeneurial ambitions, during my time at the dream teams I have learned what PR can do for yourself and your project. Therefor I strive to deliver and spread a demonstration video of the oscillating propulsion system, hopefully gaining publicity and market interest enabling the beginning of a start-up in oscillating propulsion.

FINAL COMMENTS

In case your project brief needs final comments, please add any information you think is relevant.

Bibliography

[1] Hero7 field of view (fov) information. URL `https://gopro.com/help/articles/question_answer/hero7-field-of-view-fov-information`.

[2] JM Anderson, K Streitlien, DS Barrett, and MS Triantafyllou. Oscillating foils of high propulsive efficiency. *Journal of Fluid Mechanics*, 360:41–72, 1998.

[3] Intesaaf Ashraf, Hanaé Bradshaw, Thanh-Tung Ha, José Halloy, Ramiro Godoy-Diana, and Benjamin Thiria. Simple phalanx pattern leads to energy saving in cohesive fish schooling. *Proceedings of the National Academy of Sciences*, 114(36):9599–9604, 2017.

[4] Richard Bainbridge. The speed of swimming of fish as related to size and to the frequency and amplitude of the tail beat. *Journal of experimental biology*, 35(1):109–133, 1958.

[5] Richard James Clapham and Huosheng Hu. isplash-i: High performance swimming motion of a carangiform robotic fish with full-body coordination. In *2014 IEEE International Conference on Robotics and Automation (ICRA)*, pages 322–327. IEEE, 2014.

[6] Richard James Clapham and Huosheng Hu. isplash: Realizing fast carangiform swimming to outperform a real fish. In *Robot Fish*, pages 193–218. Springer, 2015.

[7] Richard James Clapham and Huosheng Hu. isplash-optimize: Optimized linear carangiform swimming motion. In *Intelligent Autonomous Systems 13*, pages 1257–1270. Springer, 2016.

[8] Christophe Eloy. Optimal strouhal number for swimming animals. *Journal of Fluids and Structures*, 30:205–218, 2012.

[9] JOHN H HEBRANK, MARY R HEBRANK, JOHN H LONG, BARBARA A BLOCK, and STEPHEN A WRIGHT. Backbone mechanics of the blue marlin makaira nigricans (pisces, istiophoridae). *Journal of Experimental Biology*, 148(1):449–459, 1990.

[10] FS Hover, Ø Haugsdal, and MS Triantafyllou. Effect of angle of attack profiles in flapping foil propulsion. *Journal of Fluids and Structures*, 19(1):37–47, 2004.

[11] G Iosilevskii and D Weihs. Speed limits on swimming of fishes and cetaceans. *Journal of The Royal Society Interface*, 5(20):329–338, 2007.

[12] Yongnan Jia and Long Wang. Experimental implementation of distributed flocking algorithm for multiple robotic fish. *Control Engineering Practice*, 30:1–11, 2014.

[13] Alfred Cotterill Kermode. *Mechanics of Flight*. Longman, 1987.

[14] Lauder Lab. Trout (deceased) karman gait, 2009. URL `https://youtu.be/GtuHgl35TT4`.

[15] George V Lauder, Peter GA Madden, Rajat Mittal, Haibo Dong, and Meliha Bozkurttas. Locomotion with flexible propulsors: I. experimental analysis of pectoral fin swimming in sunfish. *Bioinspiration & Biomimetics*, 1(4):S25, 2006.

[16] Michael J Lighthill. Aquatic animal propulsion of high hydromechanical efficiency. *Journal of Fluid Mechanics*, 44(2):265–301, 1970.

[17] CC Lindsey. Form, function, and locomotory habits in fish. in “fish physiology. vol. vii. locomotion”(hoar, ws, and randall, dj, eds.), 1978.

[18] Stefano Marras, Takuji Noda, John F Steffensen, Morten BS Svendsen, Jens Krause, Alexander DM Wilson, Ralf HJM Kurvers, James Herbert-Read, Kevin M Boswell, and Paolo Domenici. Not so fast: swimming behavior of sailfish during predator–prey interactions using high-speed video and accelerometry. *Integrative and comparative biology*, 55(4):719–727, 2015.

[19] Anirban Mazumdar, Pablo Valdivia Y Alvarado, and Kamal Youcef-Toumi. Maneuverability of a robotic tuna with compliant body. In *2008 IEEE International Conference on Robotics and Automation*, pages 683–688. IEEE, 2008.

[20] Graham K Taylor, Robert L Nudds, and Adrian LR Thomas. Flying and swimming animals cruise at a strouhal number tuned for high power efficiency. *Nature*, 425(6959): 707, 2003.

[21] Samuel William Tolkoff. *Robotics and power measurements of the RoboTuna*. PhD thesis, Massachusetts Institute of Technology, 1999.

[22] George S Triantafyllou, MS Triantafyllou, and MA Grosenbaugh. Optimal thrust development in oscillating foils with application to fish propulsion. *Journal of Fluids and Structures*, 7(2):205–224, 1993.

[23] Michael S Triantafyllou and George S Triantafyllou. An efficient swimming machine. *Scientific american*, 272(3):64–70, 1995.

[24] Johannes Jozef Videler. On the interrelationships between morphology and movement in the tail of cichlid fish tilapia nilotica (l.). 1975.

[25] John J Videler. *Fish swimming*. Springer Science & Business Media, 2012.

[26] Daniel Weihs. Stability versus maneuverability in aquatic locomotion. *Integrative and Comparative Biology*, 42(1):127–134, 2002.

[27] Hans V Westerhoff and Karel Van Dam. *Thermodynamics and control of biological free-energy transduction*. Elsevier Science Ltd, 1987.

[28] Pablo Valdivia y Alvarado and Kamal Youcef-Toumi. Modeling and design methodology of an efficient underwater propulsion system. In *Robotics and Applications*, pages 161–166, 2003.

[29] Yong Zhong, Zheng Li, and Ruxu Du. A novel robot fish with wire-driven active body and compliant tail. *IEEE/ASME Transactions on Mechatronics*, 22(4):1633–1643, 2017.